



DEEPATLAS

Report

Hyperspectral Imaging Fault Matter 2.0 Project K06-04; K05-05 Wells

CLIENT: TNO

WELLS: K06-04; K05-05

DATE: 07-06-2023

PREPARED BY: T. Kelsay

Executive Summary

TNO showed interest in applying Deep Atlas' short-wave hyperspectral imaging technique to their Fault Matter 2.0 project -- WP 2.3 (GemFa) Geomechanical experimental analysis. 10m of core from the K06-04 and K05-05 wells were imaged. Image acquisition took place on May 24th 2023 at the Deep Atlas laboratory in Groningen.

From the rock samples provided, a set of high-quality short-wave infrared images were taken with a pixel resolution of 200µm. Images representing analyses of specific characteristics of intergranular minerals, such as the White Mica composition, Fe content, water content, and Illite/Kaolinite ratio were compiled. The results of the different analyses were interpreted in a Mineral Map showing the dominant mineral present in each pixel of the sample image.

The Mineral Maps indicate that, on the whole, both wells have varying clay content, dominated by Kaolinite with an Illite contribution. Trace amounts of Dolomite and Montmorillonite occur in well K06-04, with localized high concentrations of Dolomite in several fracture veins. Trace amounts of Al-poor Illite are present in both wells.

The noted sample of interest, depth 3850.64mAHD to 3851.00mAHD of well K06-04, has distinct zones alternating between Illite and Kaolinite dominated concentrations, with Kaolinite tending to be the most dominant throughout the sample. The clay content of this section was some of the highest in the well. The sample was measured three times, once on the flat slabbed surface, then twice more on the backside in an effort to better image the fault/fracture surface (referred to as Reverse #1 and Reverse #2 in Figures 19 and 20 of Appendix 2).

The results of this imaging project are delivered to TNO in the form of this report, the individual images used in the analysis, the LAS files for input in reservoir modelling software, a table with results, and a summary log.

Contents

Executive Summary	1
Contents	2
1. Introduction.....	3
2. Project Definition and Deliverables.....	4
3. Hyperspectral Imaging	5
3.1. Parameters and Conditions	5
3.2. Analysis Method and Workflow	6
3.3. Core Description	9
4. Results.....	10
4.1. Mineralogy Imaging	10
4.1.1. K06-04.....	11
4.1.2. K5-05.....	11
4.2. Quality Assurance	12
4.3. Deliverables	12
5. Discussion.....	13
5.1. Mineralogy Interpretation	13
5.2. Spectral Comparison	14
5.3. Implementation of Deliverables	17
6. Conclusions	18
Appendix 1: Mineralogy Logs Well K06-04 and K05-05.....	19
Appendix 2: Hyperspectral Images K06-04.....	22
Appendix 3: Hyperspectral Images K05-05.....	44

1. Introduction

TNO showed interest in mineral imaging as provided by Deep Atlas for their Fault Matter 2.0 project. In this report, Deep Atlas presents the results of the mineral imaging performed on May 24th 2023.

For this project, the mineralogy of the selected core was imaged in detail and exported in a meaningful way. Imaging, processing, and analysis of the K06-04 and K05-05 cores were done by Deep Atlas at its laboratory in Groningen.

A list of terms and explanations is provided below.

Terminology / spectral parameter	Explanation
1300-1600 nm wavelength range	This range contains OH-related absorption features that are typical of phyllosilicates and other OH-containing minerals. Classification of deepest absorption features leads to maps "1300-1600nm classified."
1650-1850 nm wavelength range	This range contains absorption features of sulphates such as Gypsum, Alunite and Jarosite. Classification of deepest absorption features leads to maps "1650-1850nm classified."
1850-2100 nm wavelength range	This range contains hydroxyl and water absorption features. Hydrated minerals have an expression in this range, including free water. Classification of deepest absorption features leads to maps "1850-2100nm classified."
2100-2400 nm wavelength range	This range contains diagnostic absorption features of a range of hydrated minerals, including clays, carbonates, and several types of sulphates. Al-rich phyllosilicates such as Muscovite, Illite, Smectite and Kaolinite have absorption features near 2200 nm. Classification of deepest absorption features leads to mineral maps "2100-2400nm classified."
Albedo	Mean reflectance value. In this study in the wavelength range between 1000 and 2500 nm.
Clay	Fine-grained minerals, including Muscovite, Illite, Smectite and Kaolinite. Strictly speaking Muscovite is not a clay but a white mica.
Fe(rous)-drop	The spectral slope between 1310 and 1600 nm, calculated by the band ratio R1600/R1310nm, indicative of Ferrous minerals.

HypPy	Hyperspectral Python. Hyperspectral processing and analysis software based on Python modules. Programmed by Wim Bakker of faculty of ITC (University of Twente).
Illite crystallinity	The ratio of the depths of the Al-OH feature near 2200 nm and the water feature near 1900 nm. Measure for the amount of water and ordering of the Muscovite-Illite-Smectite crystals.
Illite/kaolinite	The relative proportion of Illite versus kaolinite based on the spectral ratio of bands b2178/b2189. Higher values indicate higher proportions of Illite relative to Kaolinite. Band ratio adapted for the relative proportions of Illite versus Dickite and Nacrite
Wavelength map	A map showing, for a specific wavelength range, the wavelength position of the deepest absorption feature in colour and the depth of the same feature as intensity. Such a map provides a quick overview of the positions and relative depths of absorption features.
White mica	In this study the term refers to Muscovite and Illite
White mica composition	This term is used in reference to the occupancy of Al in octahedral sites in white micas and Al-clay minerals. The higher the occupancy, the lower the absorption wavelength of the absorption feature near 2200 nm. Change in Al-content is often the result of the coupled Tschermak substitution, a coupled substitution by Fe and Mg by Al in octahedral sites.

2. Project Definition and Deliverables

The objective of the Fault Matter 2.0 project is to deliver mineral imaging results through the interpretation method developed by Deep Atlas. TNO provided access to 10m of core from the K06-04 and K05-05 wells.

The deliverables of the Hyperspectral Imaging Fault Matter 2.0 project are:

- Full report
- Image files of every section (Albedo/R1650nm, Fe Drop, White Mica composition, Illite Crystallinity, Illite/Kaolinite, Clay content, Mineral Map)
- LAS files

- Mineralogy Log (<2185nm, Montmorillonite, Kaolinite, Illite, Illite Crystallinity, Illite/Kaolinite, Clay content, Mineral Map)
- Raw imaging data

3. Hyperspectral Imaging

Deep Atlas uses hyperspectral imaging in the short-wave infrared domain (1000nm – 2500nm) to identify what (clay) minerals are present in the core samples. In hyperspectral imaging, each pixel contains a spectrum indicating the reflectance per wavelength (nm). Molecular bonds in the mineral structure absorb (infrared) light at specific wavelengths (Figure 1). This absence of reflectivity at these specific wavelengths is characteristic of the mineral(s) present within the pixel related to that spectrum. Minerals can thus be identified by their characteristic reflectance spectra.

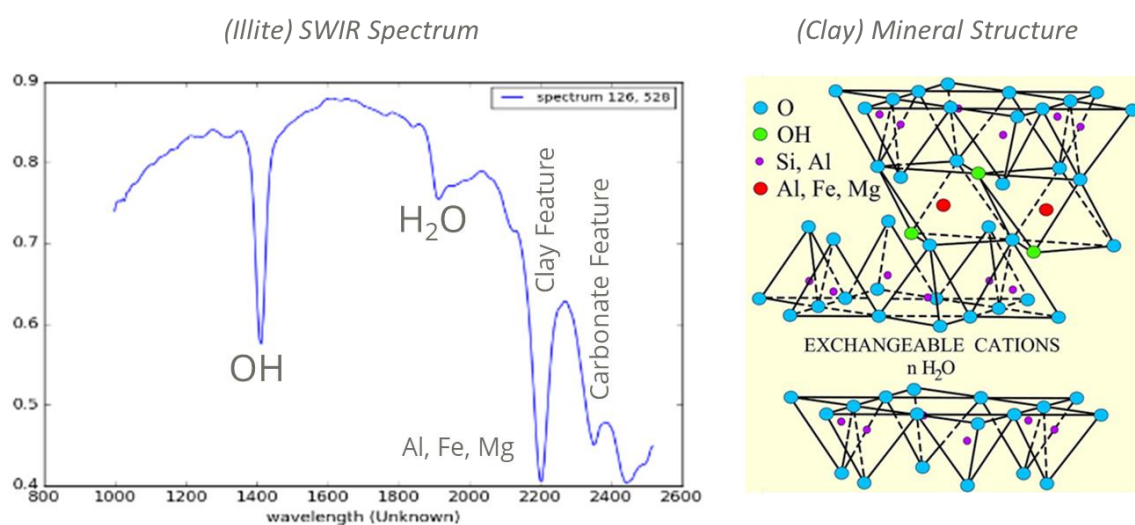


Figure 1: Example spectrum of Illite indicating what absorption peaks are caused by what molecular bonds. The molecular bond positions in the clay mineral structure are shown on the right.

3.1. Parameters and Conditions

Deep Atlas' Short Wave Infra-Red (SWIR) camera was used to acquire hyperspectral images at 0.2mm spatial resolution. The camera type is Specim SWIR-LVDS-100-N25E with a 12nm spectral resolution and 5.6nm spectral sampling in 272 bands. The camera has a

spectral range of 1000nm-2500nm ideal for identifying clay- and carbonate minerals and their polymorphs. The camera can measure samples up to 1m in length.

The core (K06-04 (9m); K05-05(1m)) was measured at Deep Atlas' laboratory in Groningen on May 24th 2023. Imaging took place in a dedicated laboratory without direct sunlight and few additional light sources.

The Specim SWIR camera was not connected to the internet during the scanning campaign and data transfer to the database was done by disk to a computer in the office environment in Groningen. The data was transferred to the database, where the automated processing and interpretation steps were initiated.



Figure 2: SWIR Hyperspectral camera setup in Deep Atlas' Lab in Groningen.

Deep Atlas uses Target Field Lab's (University Groningen) services for data handling and storage. The data is stored in a secure location under the control of the University Groningen. The data generated in this study will not be distributed to 3rd parties without the core owner's approval.

3.2. Analysis Method and Workflow

Deep Atlas developed, in collaboration with the ITC Faculty of the University of Twente, a workflow capable of processing and interpreting hyperspectral data generated by the Specim SWIR camera (Figure 3). The workflow uses HypPy (Hyperspectral Python) software, developed by the University of Twente, which is automated by the Target Field

Lab of the University of Groningen. As this is the first project with Deep Atlas' SWIR hyperspectral camera, several components had to be calibrated to its output.

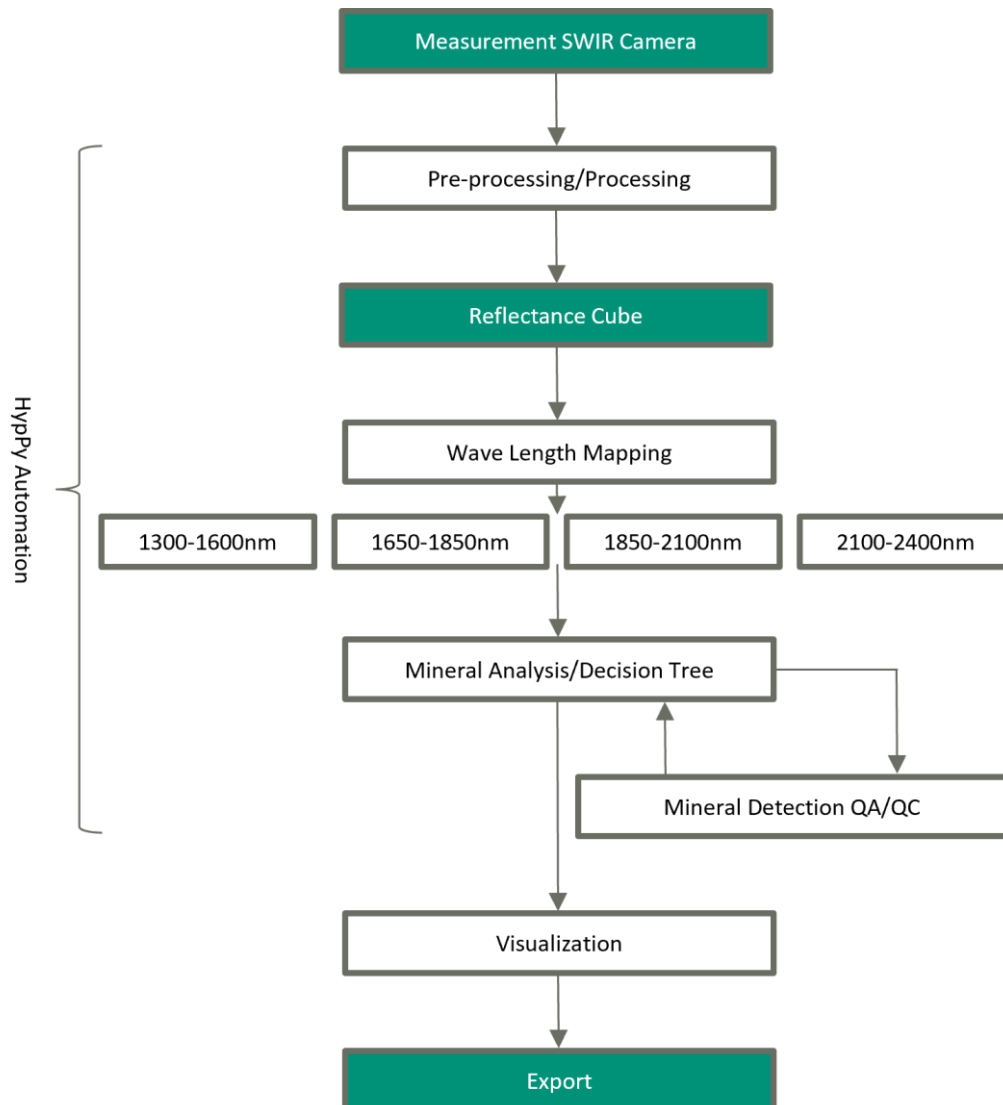


Figure 3: Schematic overview of Deep Atlas' data processing and analysis workflow.

During the Wave Length Mapping step, all spectra are subdivided into 4 segments representing specific chemical parts of (clay) minerals (e.g., Al-OH and H₂O groups) (Figure 1). In each segment, the wavelength position and depth of the 1st, 2nd, and 3rd most prominent absorption features are captured (Figure 4).

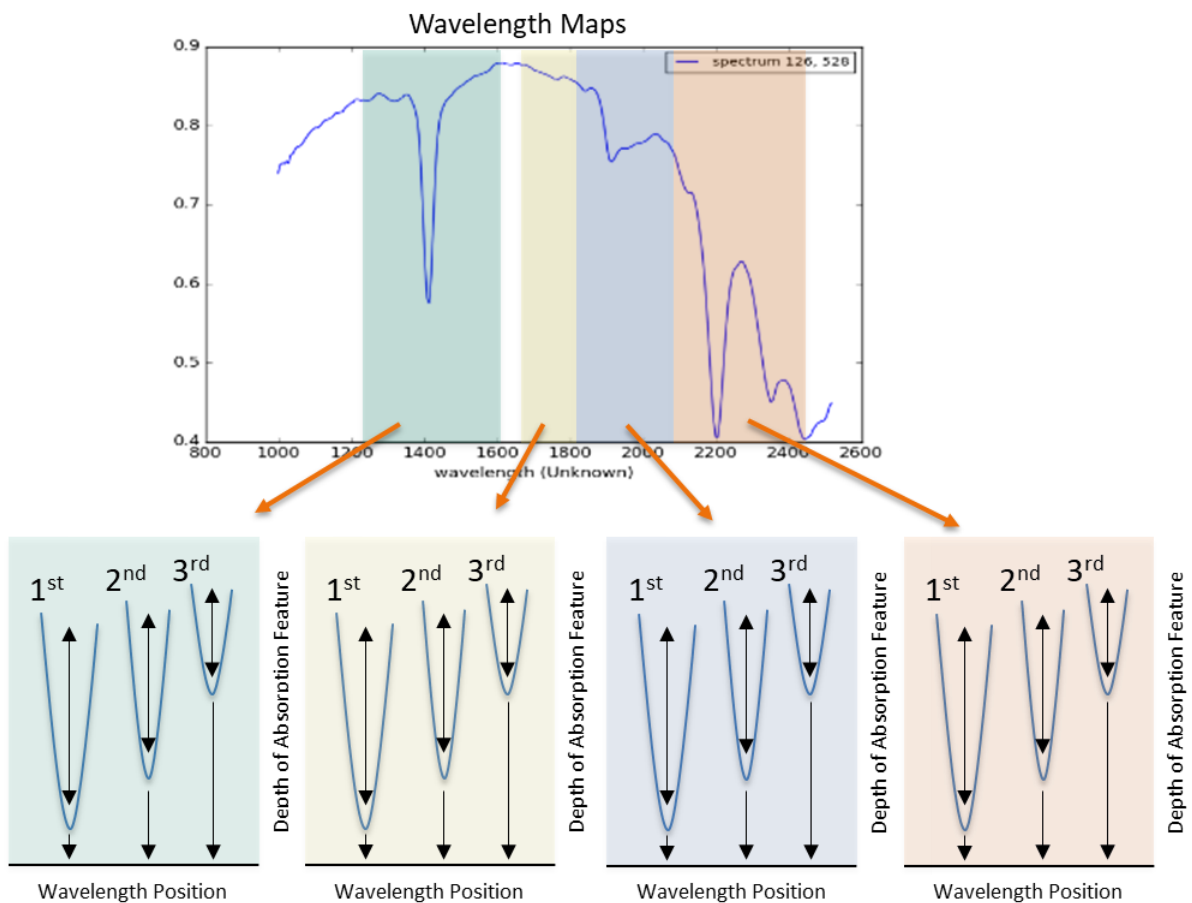


Figure 4: Wavelength mapping where each spectrum is subdivided into 4 segments, and per section the wavelength position and depth of the 1st, 2nd, and 3rd absorption features.

Classifying minerals is done by analyzing and comparing the wavelength positions and depth from all wavelength maps using decision trees. The decision trees are developed by Deep Atlas and the University of Twente. An additional QC step uses principal component analysis and linear unmixing to check the quality of the classified Mineral Map and identify pixels containing mixed mineral assemblages. In this step, the concentrations of the individual (clay) mineral species are also determined (Figure 3).

The depth of the feature is a semi-quantitative measure of the concentration of mineral(s) present within the spectrum, and thus the pixel. Deep Atlas established a relationship between the concentration of (clay) minerals, in volume percent, and the depth of the related absorption feature. This relationship was established using QEMSCAN results compared to the hyperspectral imaging results of the cut-offs.

The Mineral Maps and specific tests, like Fe-drop and Illite Crystallinity, are visualized as images and summarized as log files in LAS format. Depending on the client's request, the

images can be displayed separately or stitched together in a mineralogy log covering the entire sampling length (see Appendix 1).

Reference to Decision Trees Applied: Albedo_V3R0C082021, Fe_Drop_V3R0C082021, White_Mica_V3R0C082021, Illite_Crystallinity_V5R2C042023, Illite/Kaolinite_V5R2C042023, Clay_Content_V4R1C042023, Sedimentary_Mineralogy_v3

3.3. Core Description

TNO provided 10m of core to be measured in the Fault Matter 2.0 project. Table 1 gives an overview of the distribution of material over the two wells.

Table 1: Overview of core material per well.

Well	Core	Scans/Images	Alternate Angle Scans
K06-04	9.00mAHD	18	2
K05-05	1.00mAHD	2	0

All core was loose core, specifically the 1/3 core sections. The core sections were of moderate-to-good quality, flat (on the face), had temporary annotations, attached with adhesive stickers (removed for scanning), and had permanent annotations written directly on the core, which can affect the hyperspectral imaging in those locations. There were several broken-up sections that made minimizing variations in core height challenging, e.g., 3845.50mAHD to 3845.99mAHD and 3850.00mAHD to 3850.50mAHD of well K06-04. Variations in core height larger than 1-2 cm might lead to (slightly) unsharp images of the core surface (measured surface); however, unsharp images still contain the spectral information required to make interpretations. Research on this topic, in collaboration with the University of Twente, concluded that the spectral information is of sufficient quality to make correct interpretations. No low-resolution RGB photos were taken from each slabbed core interval; as TNO specified, this was completed prior to delivery. The loose core was stored in cardboard boxes with polystyrene foam spacers. Core surfaces were cleaned by TNO prior to delivery to Deep Atlas' laboratory in Groningen.

4. Results

The available dataset was imaged and analyzed between May 24th and June 7th 2023. In this section, the mineral imaging results are described. Reference will be made to Appendix 1 to 3, where the products per image are displayed and the mineralogy log is presented. The reference to the appendices is made to keep the report readable.

4.1. Mineralogy Imaging

The figures in Appendix 2 and 3 show the hyperspectral imaging results as interpreted by Deep Atlas. Mineralogy parameters such as Fe content, White Mica composition, Illite/Kaolinite ratio, Illite Crystallinity, and clay content are helpful parameters to visualize this variation. General observations and comments are listed below.

Composition

The clay mineralogy in well K06-04 is dominated by Kaolinite with an Illite contribution. The clay mineralogy in well K05-05 is dominated by Illite with a strong Kaolinite contribution. K6-04 has trace amounts of Dolomite and Montmorillonite and a noticeably higher Kaolinite contribution. There are slight variations in composition on a cm-to-m scale. K06-04 appears to have slightly more Al-poor Illite, however, there is only one meter of comparable data from K05-05, so this may not be applicable to the entire well.

Crystallinity

The Illite Crystallinity measures the water present within the clay mineral, whereas Smectite contains more and Muscovite contain less water than Illite. Within the two wells, the overall trend of Illite Crystallinity is quite consistent, with the exception of the sample from 3850.64mAHD to 3851.00mAHD in well K06-04, where it is noticeably higher.

Clay Content

Absolute clay content numbers (vol%) are derived from relationships established by comparing quantitative QEMSCAN results to the depth of hyperspectral absorption

features of samples taken from Dutch Rotliegend reservoirs (Offshore K-blocks). There is some uncertainty around how accurate this relationship is to determining the clay content in other sandstones.

4.1.1. K06-04

The scanned core from well K06-04 extended from 3844.50mAHD to 3853.50mAHD. The K06-04 Mineralogy Log is in Appendix 1 (also available as a separate PNG image).

The well is dominated by Kaolinite with an Illite contribution and a relatively high, compared to K05-05, clay content. Trace Dolomite, Al-poor Illite, and Montmorillonite are present in the well. The intervals 3849.92mAHD to 3850.36mAHD and 3852.56mAHD to 3852.96mAHD have localized high concentrations of Dolomite in the fracture veins. The intervals 3849.50mAHD to 3850.76mAHD and 3852.56mAHD to 3853.50mAHD have consistently higher spatial variation (spatial entropy) than the rest of the well. For most of the well, the overall trend of Illite Crystallinity is consistent, with the exception of the sample from 3850.64mAHD to 3851.00mAHD and a slight step change (decrease) at 3852.56mAHD,

The sample from 3850.64mAHD to 3851.00mAHD was noted as being of particular interest. This sample has distinct zones alternating between Illite and Kaolinite dominated concentrations, with Kaolinite being the most dominant throughout the sample. The clay content of this section was some of the highest in the well. The sample was measured on the flat slabbed surface once, then again two more times on the backside in an effort to better image the fault/fracture surface (referred to as Reverse #1 and Reverse #2 in Figures 19 and 20 of Appendix 2). Initially, imaging was problematic due to the dark coloring of the smooth fault surface on the backside of the sample. To overcome this issue, adjustments were made to the background filtering algorithm for this sample.

4.1.2. K5-05

The scanned core from well K05-05 extended from 3753.54mAHD to 3754.20mAHD. The K05-05 Mineralogy Log is in Appendix 1 (also available as a separate PNG image).

Compared to K06-04, K05-05 has a relatively low Clay content. Trace Al-poor Illite is present in the well. The top half of the well, from 3753.54mAHD to 3753.82mAHD, is dominated by Illite, with an (increasing in volume) Kaolinite component. The lower half is dominated by Illite, with a (decreasing in volume) Kaolinite component.

4.2. Quality Assurance

The quality of the automatically generated images is primarily assessed visually. Deep Atlas' in-house software allows visual checks of the processed reflectance cube, the Mineral Map, and all intermediate steps. Summary spectra per image allow for control of the interpreted mineralogy.

The quality of the input images (RAW format) and the processed reflectance cubes were checked and were deemed of good quality over the actual rock samples. The automatic filter that removes resin and background spectra worked well for the whole sections of loose core, but the background for the broken-up sections of core (e.g., 3845.50mAHD to 3845.99mAHD and 3850.00mAHD to 3850.50mAHD) proved problematic for this filter. Adjustment to the automatic background filter resulted in clipped images of the loose core leaving a very limited amount of background around the rock sample.

The quality of the Mineral Map and all intermediate and side products is good. Images are clear and correctly interpreted. Besides visual checks of the entire length of the core, several core sections were analyzed in more detail to assure a correct interpretation. This was especially the case in the sample from 3850.64mAHD to 3851.00mAHD of well K06-04.

The generated deliverables were checked for completeness, correct graphical representation, and annotation.

4.3. Deliverables

Detailed processed images for the Albedo, Fe content, White Mica composition, Illite Crystallinity, Illite/Kaolinite ratio, Clay content, and Mineral Map are included per sampled interval (e.g., every half meter). The well name and depth interval are included in the filename for reference.

The LAS files used in this report and the mineralogy logs (Appendix 1) are available in a separate folder. The LAS files can be used to upload the mineralogy imaging to the subsurface and petrophysical modelling software.

The mineralogy logs (Appendix 1) provide a continuous overview of the mineralogy parameters contributing to the permeability distribution. The individual PNG images are delivered separately from this report for more detailed observations.

The raw image files were delivered to TNO on May 24th at Deep Atlas' laboratory.

5. Discussion

5.1. Mineralogy Interpretation

Figures 5 and 6 provide continuous vertical images derived from the individual interpretation images. The individual images are at a 2cm vertical interval. The interval size was chosen to still represent the geological content while at the same time providing a smoothed readable profile.

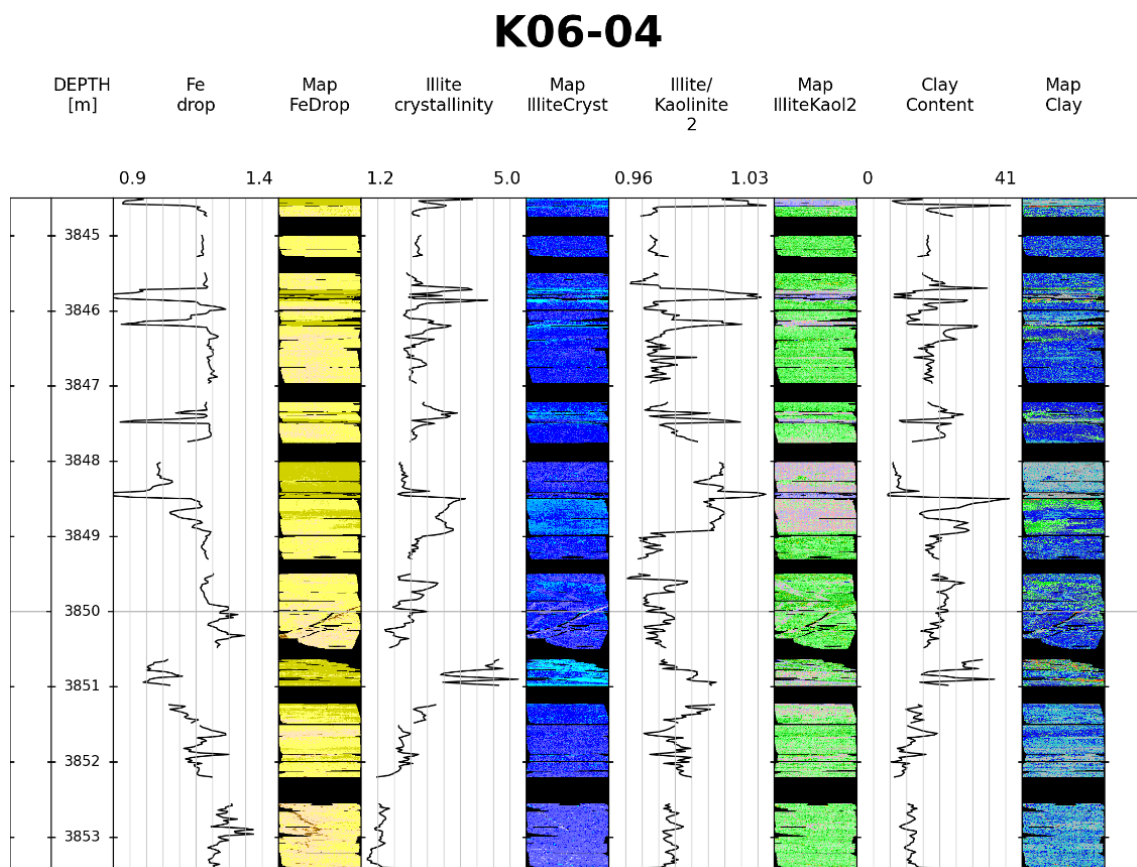


Figure 5: Overview how the derived single value LAS files relate to the summary maps of different analyses applied to well K06-04.

K05-05

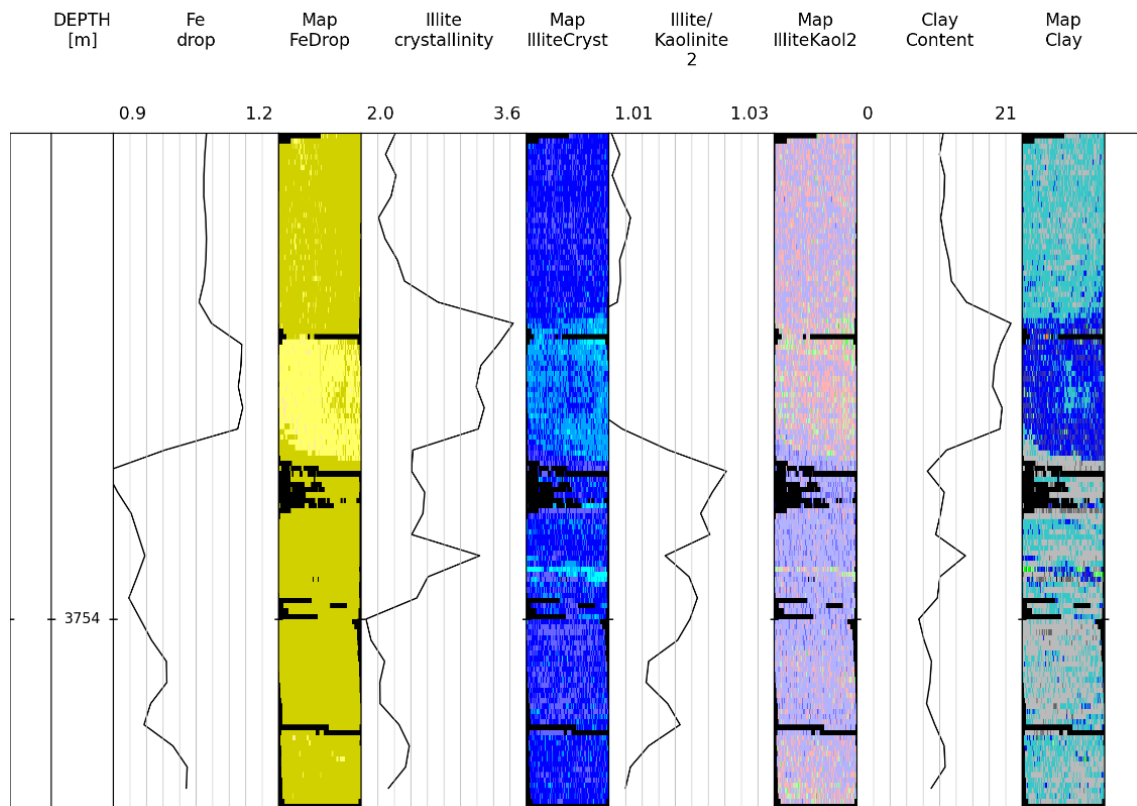


Figure 6: Overview how the derived single value LAS files relate to the summary maps of different analyses applied to well K05-05.

A structured subdivision of the reservoir into specific mineralogically similar units is outside the scope of this study. Such a subdivision would have the objective of supporting the client in defining the reservoir units in their subsurface modelling.

Figures 5 and 6 are available as separate PNG images in the accompanying dataset to this report.

5.2. Spectral Comparison

The predominant mineral in the rock matrix of both wells is Kaolinite, which exhibits a distinct absorption pattern with a double peak at 2170nm and 2210nm and 1380nm and 1410nm. There appears to be a difference in Kaolinite composition between Kaolinite present in fine-grained material and Kaolinite associated with coarse-grained sediments and fractures.

In contrast, the fractures are primarily composed of Illite, which shows single peaks at 2200nm (diagnostic) and 1410nm. A shift in this diagnostic peak for Illite can be found on the fracture surface of Reverse #1 and is related to an Al-poor Illite composition (Figure 7).

Notably, certain samples in well K06-04 display localized high concentrations of Dolomite within the fractures. Figures 8 and 9 illustrate these significant spectral variations, showcasing samples from depths ranging from 3850.00mAHD to 3850.50mAHD and 3852.56mAHD to 3853.00mAHD in well K06-04.

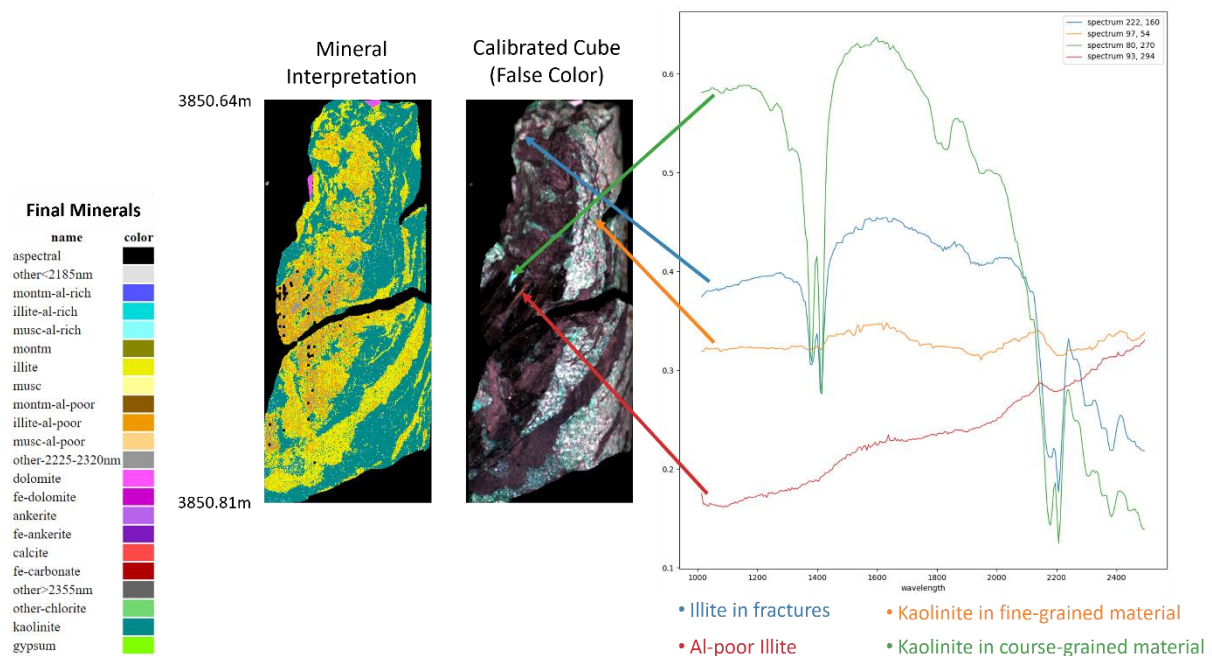


Figure 7: Spectral comparison of Reverse #1 from K06-04 3850.64mAHD to 3850.81mAHD. Clear distinction between Kaolinite dominated material (fine-grained and course-grained), Illite dominated smaller fractures, and Al-poor Illite found on the large fracture surface.

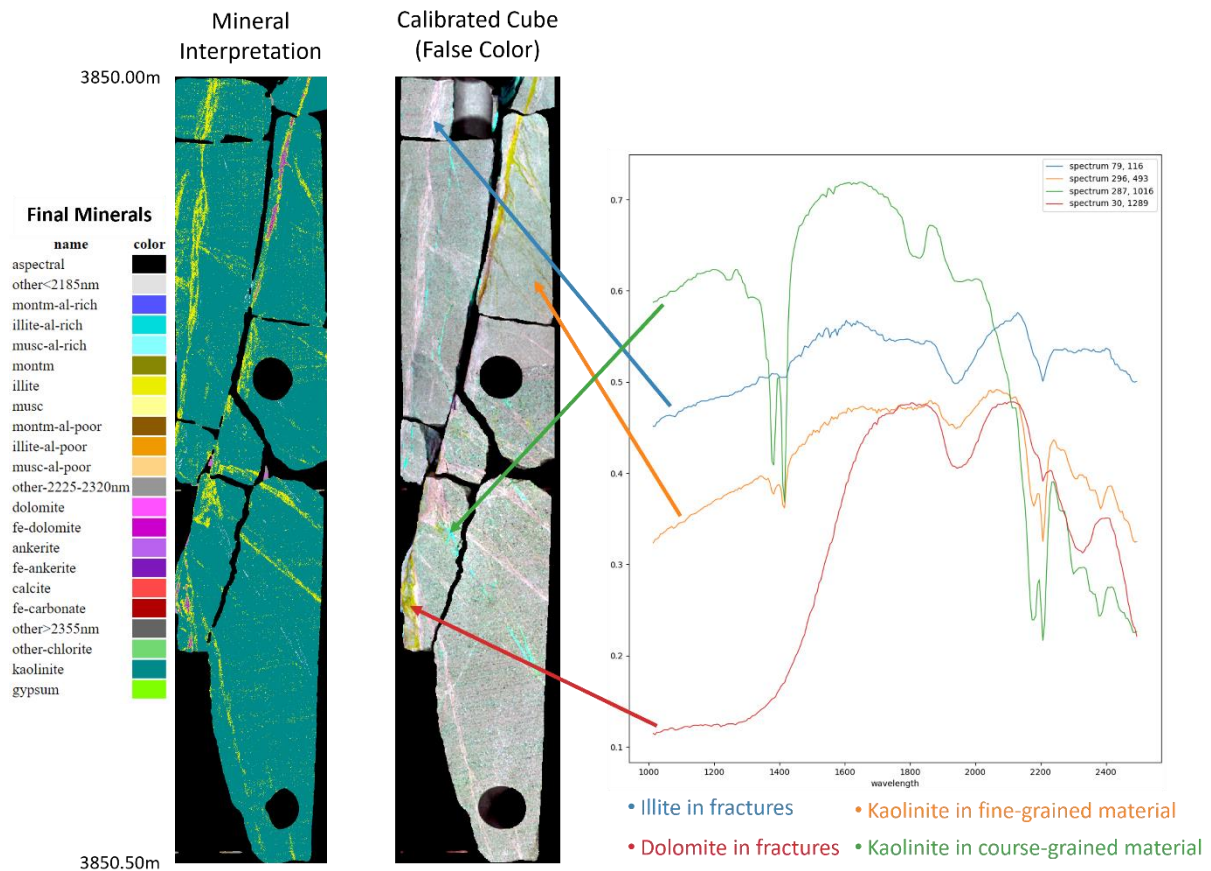


Figure 8: Spectral comparison from K06-04 3850.00mAHD to 3850.50mAHD. Clear distinction between Kaolinite dominated material (fine-grained and coarse-grained), Illite dominated fractures, and Dolomite presence in several fractures.

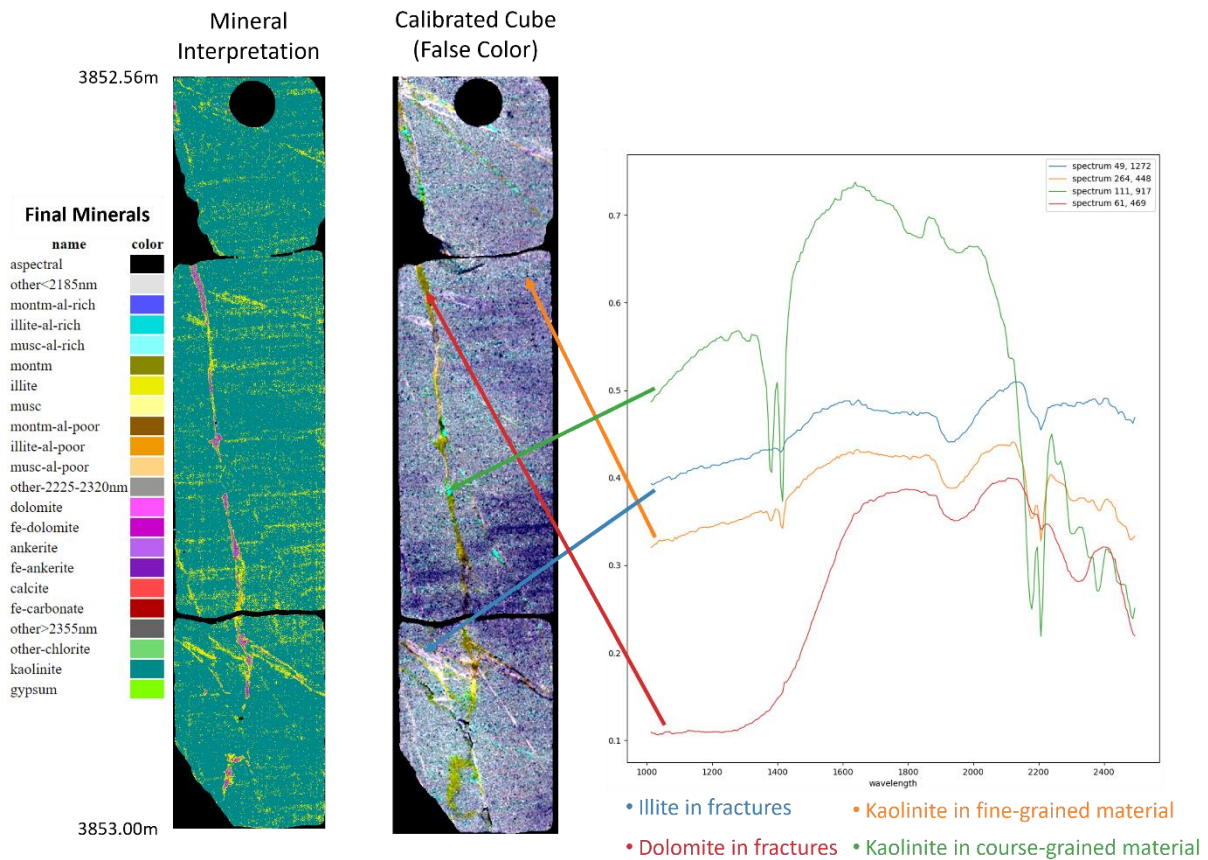


Figure 9: Spectral comparison from K06-04 3852.56m AHD to 3853.00m AHD. Clear distinction between Kaolinite dominated material (fine-grained and coarse-grained), Illite dominated fractures, and Dolomite presence in several fractures.

5.3. Implementation of Deliverables

The information compiled in the LAS files, images, and mineralogy log gives valuable insight into the character and volume of pore-filling minerals, such as clay minerals and carbonates. However, due to the lack of absorption features in the short-wave infrared light for Quartz and Feldspar, dominant rock-forming minerals in sedimentary rocks, the matrix is not included in the interpretation.

In reservoir characterization, mineral imaging results are highly recommended to be analyzed relative to, and in combination with, other sources of information (e.g., well log data (GR and Neutron Density) and detailed laboratory results). The provided LAS files allow for easy incorporation of mineralogy information into subsurface or petrophysical software. It should be kept in mind that the LAS files represent an average over a small (cm scale) interval. Qualitative detailed understanding of the reservoir character, e.g.,

upsampling parameter decisions or facies analysis, can be obtained from the provided images.

6. Conclusions

The quality of the loose core samples was suitable to perform the hyperspectral imaging, as outlined in this report. Processing and interpreting the dataset resulted in a set of topic-specific images with a 200 μ m resolution. Visual quality checks confirmed the high-quality of the image and the interpretation.

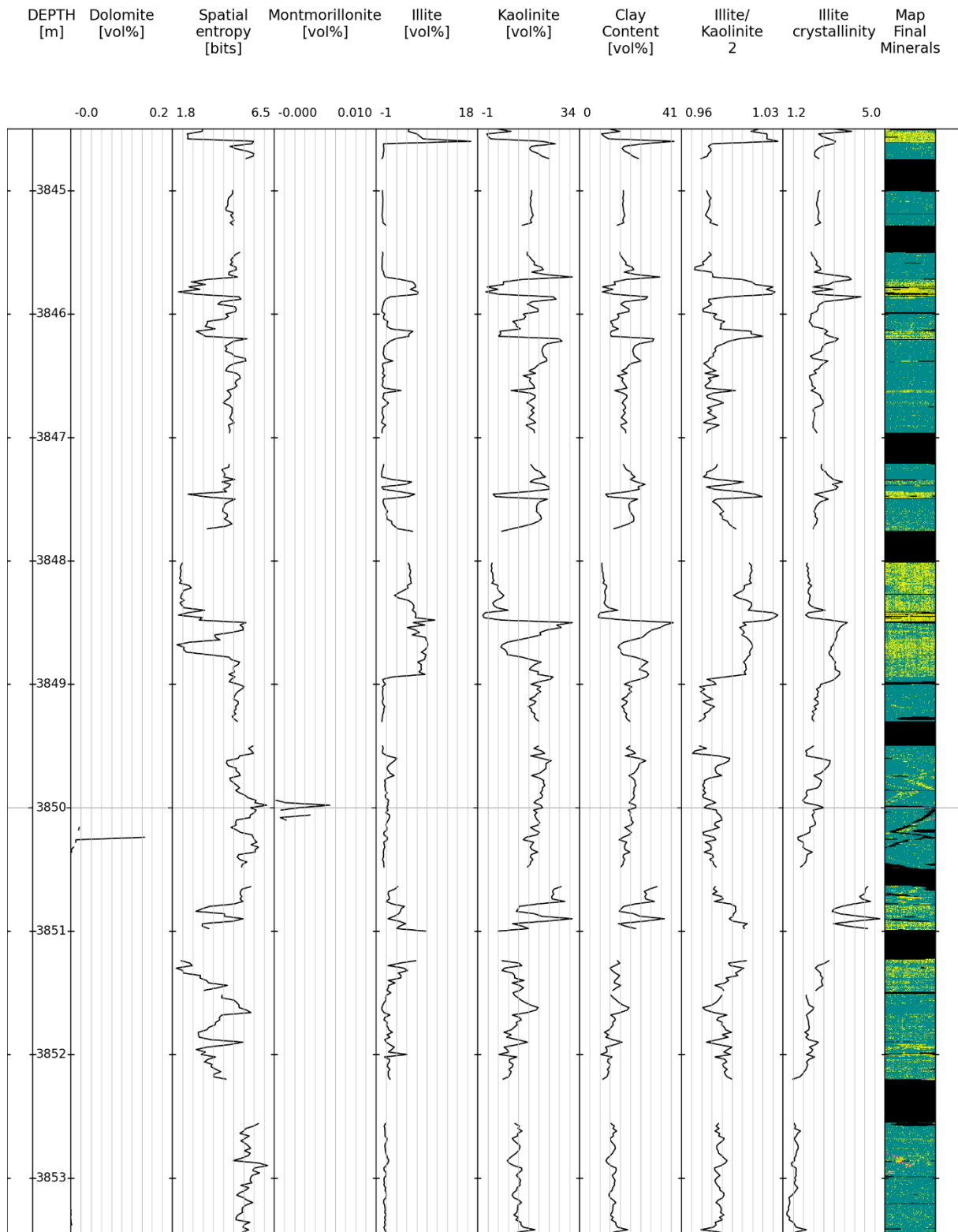
On the whole, both wells have varying clay content, dominated by Kaolinite with an Illite contribution. Trace amounts of Dolomite and Montmorillonite occur in well K06-04, with localized high concentrations of Dolomite in several fracture veins. Trace amounts of Al-poor Illite are present in both wells.

The noted sample of interest, depth 3850.64mAHD to 3851.00mAHD of well K06-04, has distinct zones alternating between Illite and Kaolinite dominated concentrations, with Kaolinite tending to be the most dominant throughout the sample. The clay content of this section was some of the highest in the well. The sample was measured three times, once on the flat slabbed surface, then twice more on the backside in an effort to better image the fault/fracture surface (referred to as Reverse #1 and Reverse #2 in Figures 19 and 20 of Appendix 2). Initially, imaging was problematic due to the dark coloring of the smooth fault surface on the backside of the sample. To overcome this issue, adjustments were made to the background filtering algorithm for this sample.

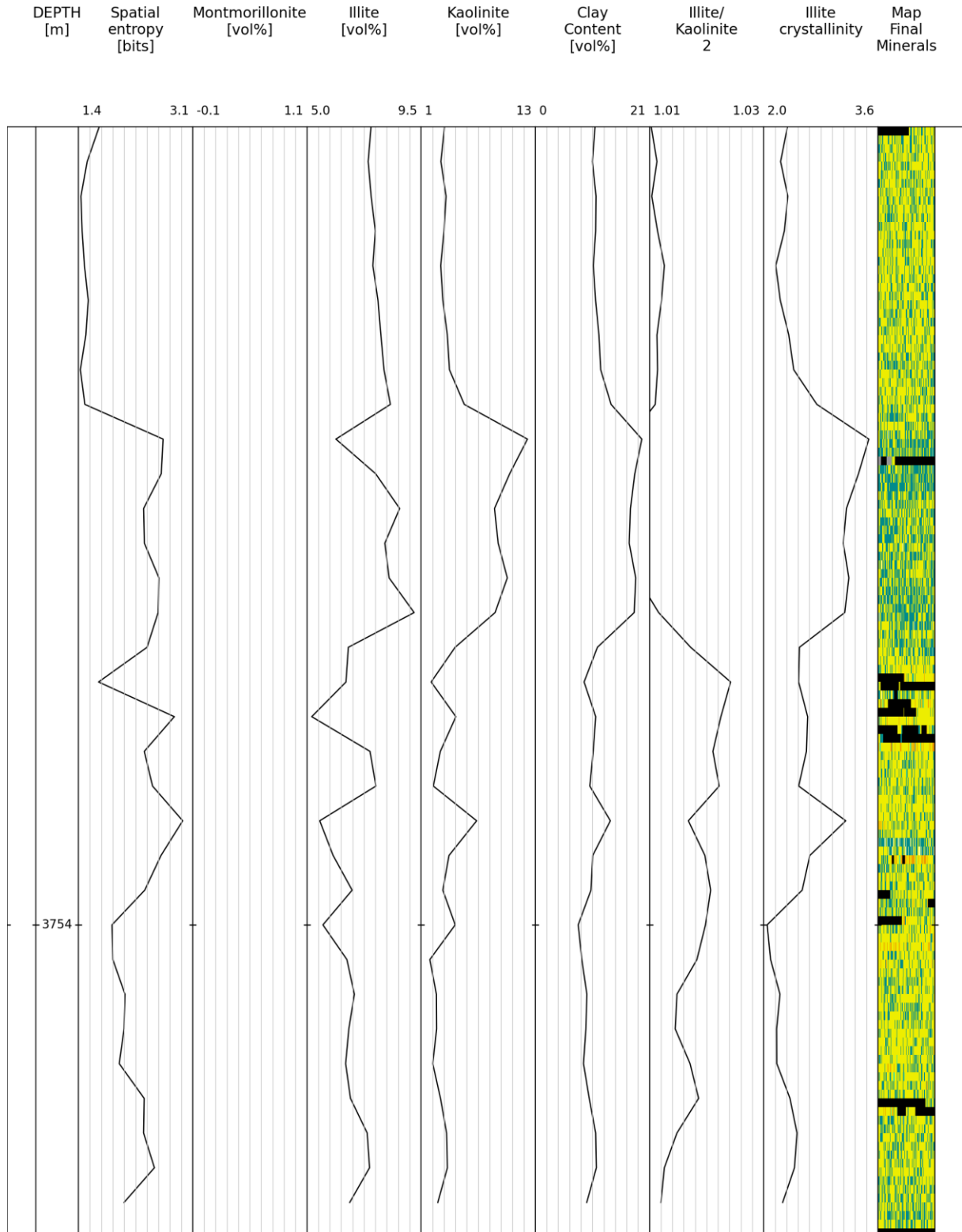
Appendix 1: Mineralogy Logs Well K06-04 and K05-05

Note that K06-04 and K05-05 Mineralogy Logs are provided as separate PNG images in the accompanying dataset for more detailed observations.

K06-04











K05-05









Appendix 2: Hyperspectral Images K06-04

Legend











Fe Drop

name	color
fed-aspectral	
fed-no2100-2400	
fed-low	
fed-med-low	
fed-medium	
fed-med-high	
fed-high	
fed-very-high	

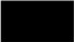

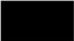

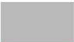



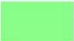










White Mica Composition

name	color
wm-aspectral	
2-LT2185	
wm-LT2190	
wm-LT2190_w2	
wm-LT2195	
wm-LT2195_w2	
wm-LT2200	
wm-LT2200_w2	
wm-LT2205	
wm-LT2205_w2	
wm-LT2210	
wm-LT2210_w2	
wm-LT2215	
wm-LT2215_w2	
wm-LT2220	
wm-LT2220_w2	
wm-LT2225	
wm-LT2225_w2	
wm-GT2225	






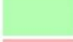




Illite Crystallinity

name	color
ix-aspectral	
ix-NO-ALOH	
ix-smect3	
ix-smect2	
ix-smect1	
ix-smect-ill	
ix-ill-smect	
ix-hx-ill	
ix-musc1	
ix-musc2	

Clay Content (vol%)

name	color
cc-aspectral	
cc-no-ALOH	
cc-0-1	
cc-1-5	
cc-5-10	
cc-10-15	
cc-15-20	
cc-20-25	
cc-25-30	
cc-30-35	
cc-35-40	
cc-40-45	
cc-45-50	
cc-50-60	
cc-60-70	
cc-70-80	
cc-80-90	
cc-90-100	
cc-GT100	

Illite/Kaolinite

name	color
ik-aspectral	
ik-NO-ALOH	
ik-kaol4	
ik-kaol3	
ik-kaol2	
ik-kaol1	
ik-ill1	
ik-ill2	
ik-ill3	
ik-ill4	

Final Minerals

name	color
aspectral	
other<2185nm	
montm-al-rich	
illite-al-rich	
musc-al-rich	
montm	
illite	
musc	
montm-al-poor	
illite-al-poor	
musc-al-poor	
other-2225-2320nm	
dolomite	
fe-dolomite	
ankerite	
fe-ankerite	
calcite	
fe-carbonate	
other>2355nm	
other-chlorite	
kaolinite	
gypsum	

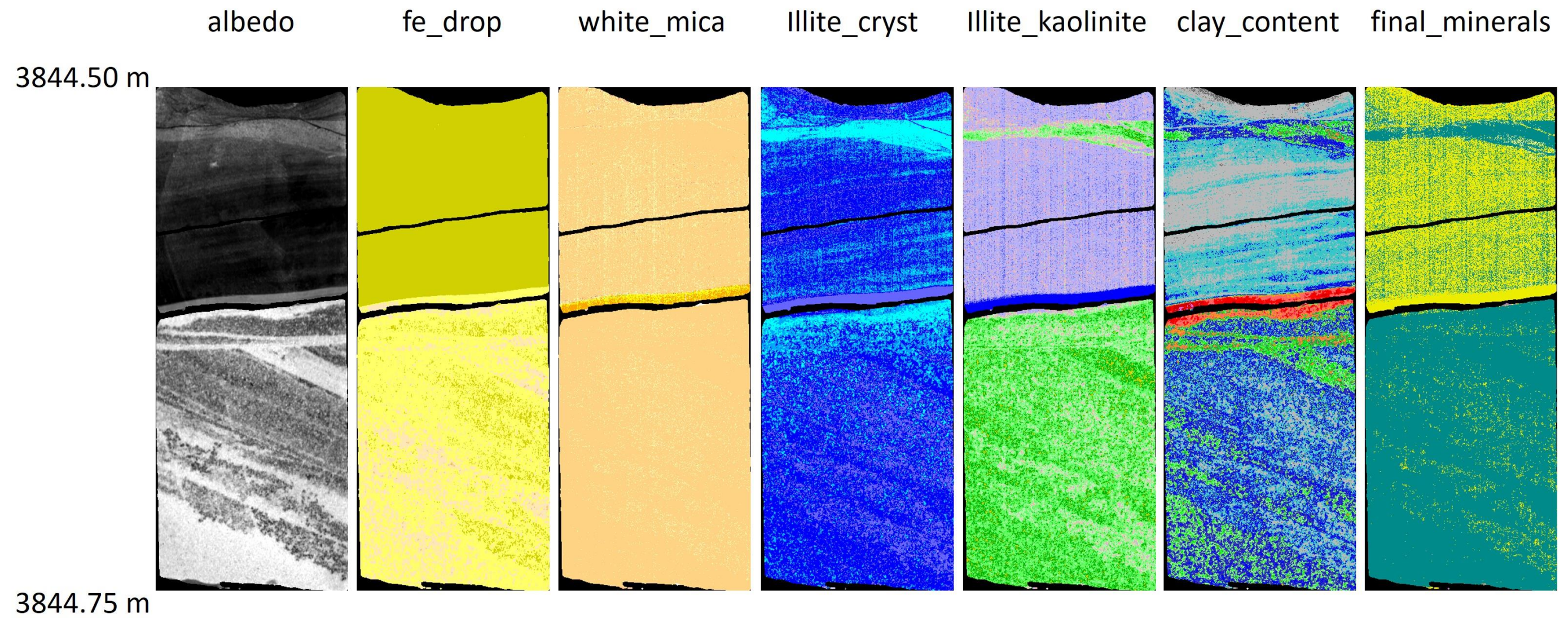


Figure 1: Mineral Map and specific/intermediate tests to understand the character and quantity of the mineral distribution between 3844.50m and 3844.75m.

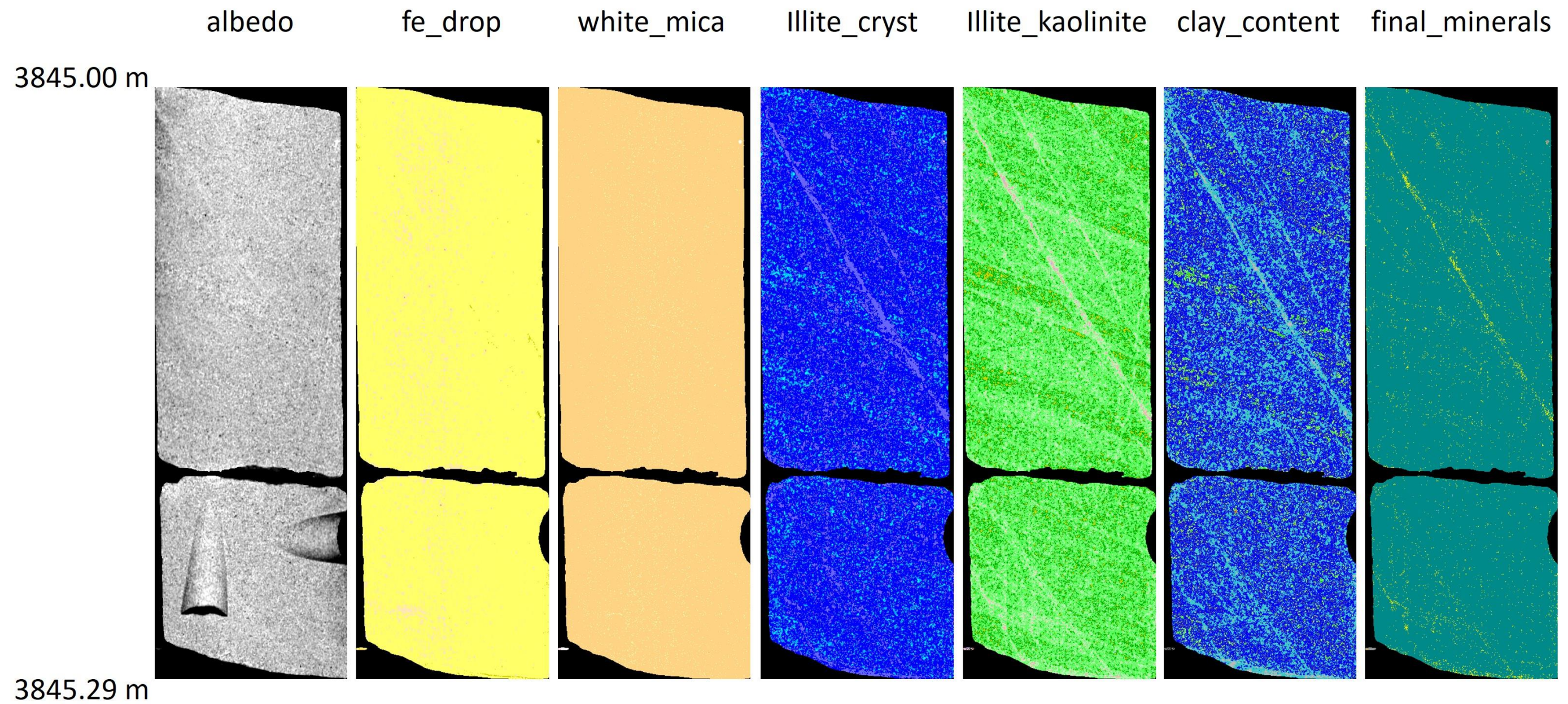


Figure 2: Mineral Map and specific/intermediate tests to understand the character and quantity of the mineral distribution between 3845.00m and 3845.29m.

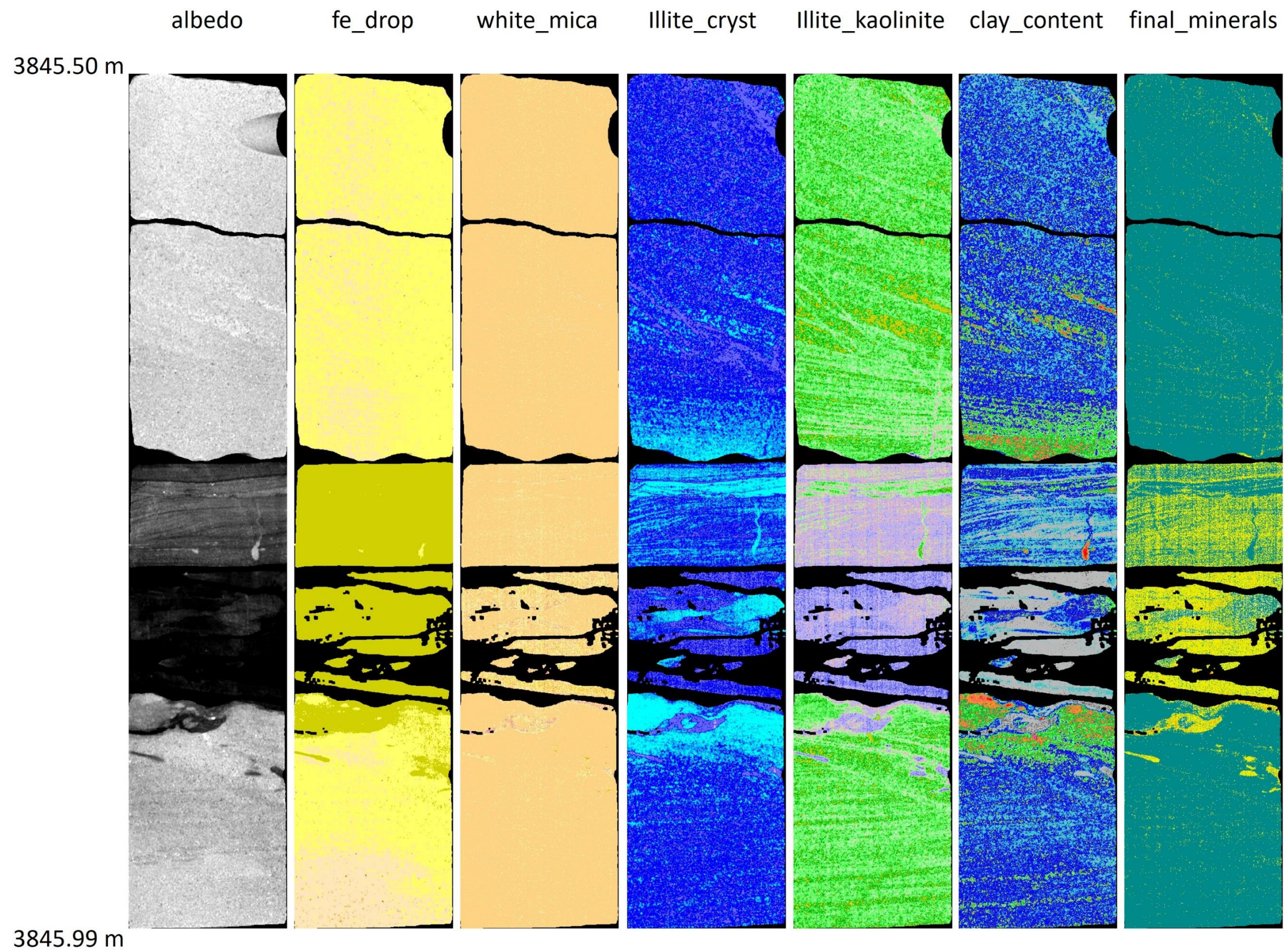


Figure 3: Mineral Map and specific/intermediate tests to understand the character and quantity of the mineral distribution between 3845.50m and 3845.99m.

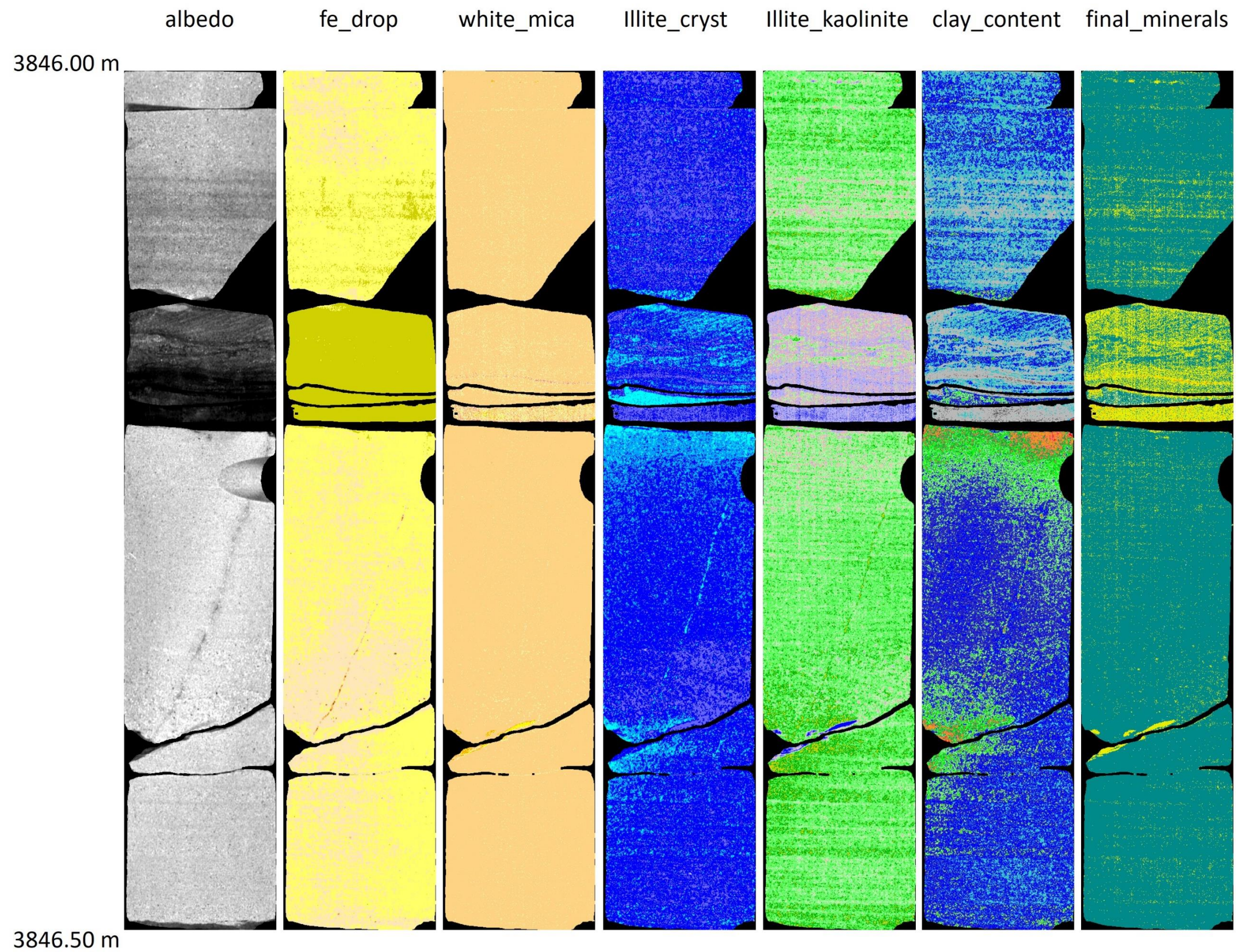


Figure 4: Mineral Map and specific/intermediate tests to understand the character and quantity of the mineral distribution between 3846.00m and 3846.50m.

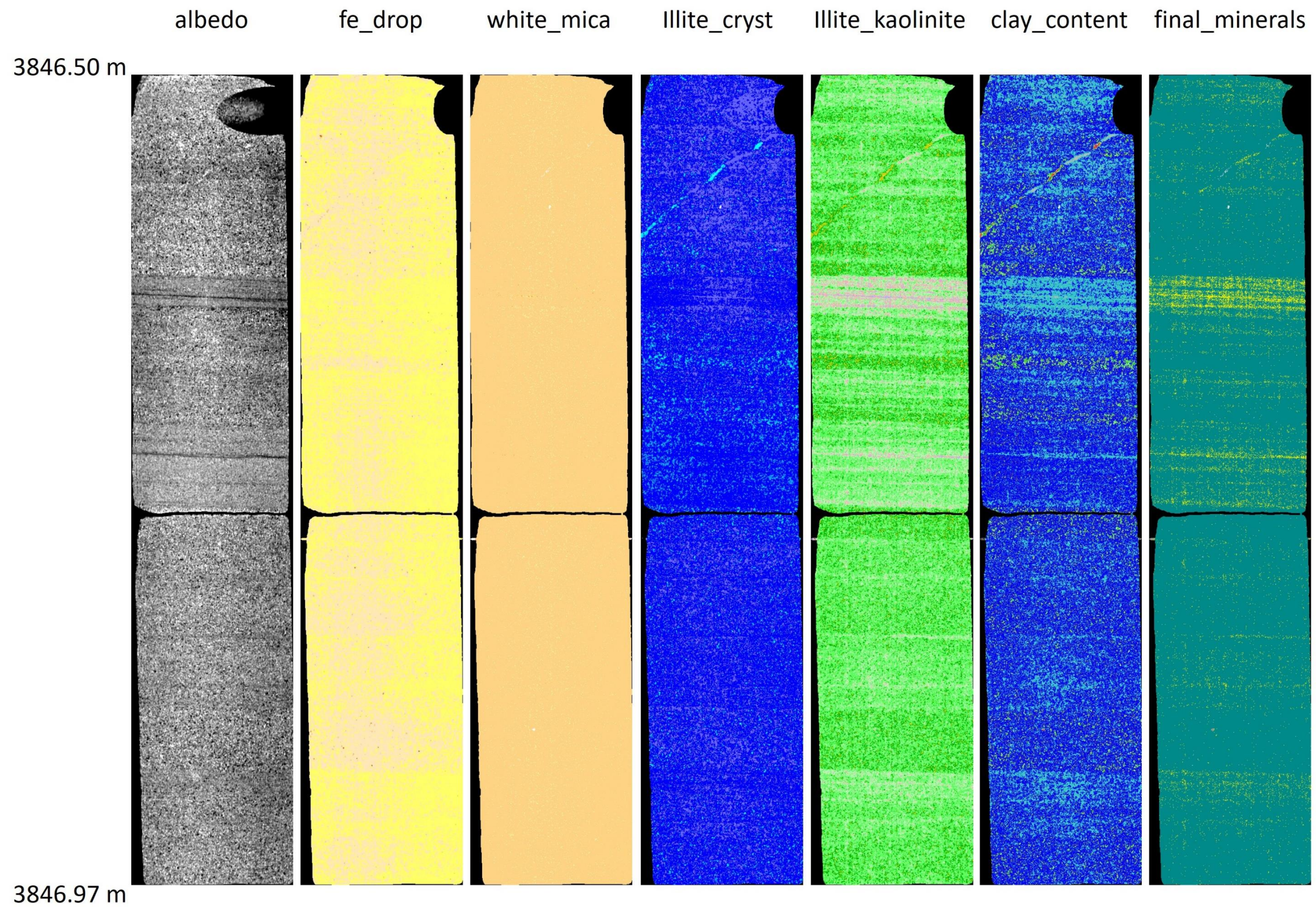


Figure 5: Mineral Map and specific/intermediate tests to understand the character and quantity of the mineral distribution between 3846.50m and 3846.97m.

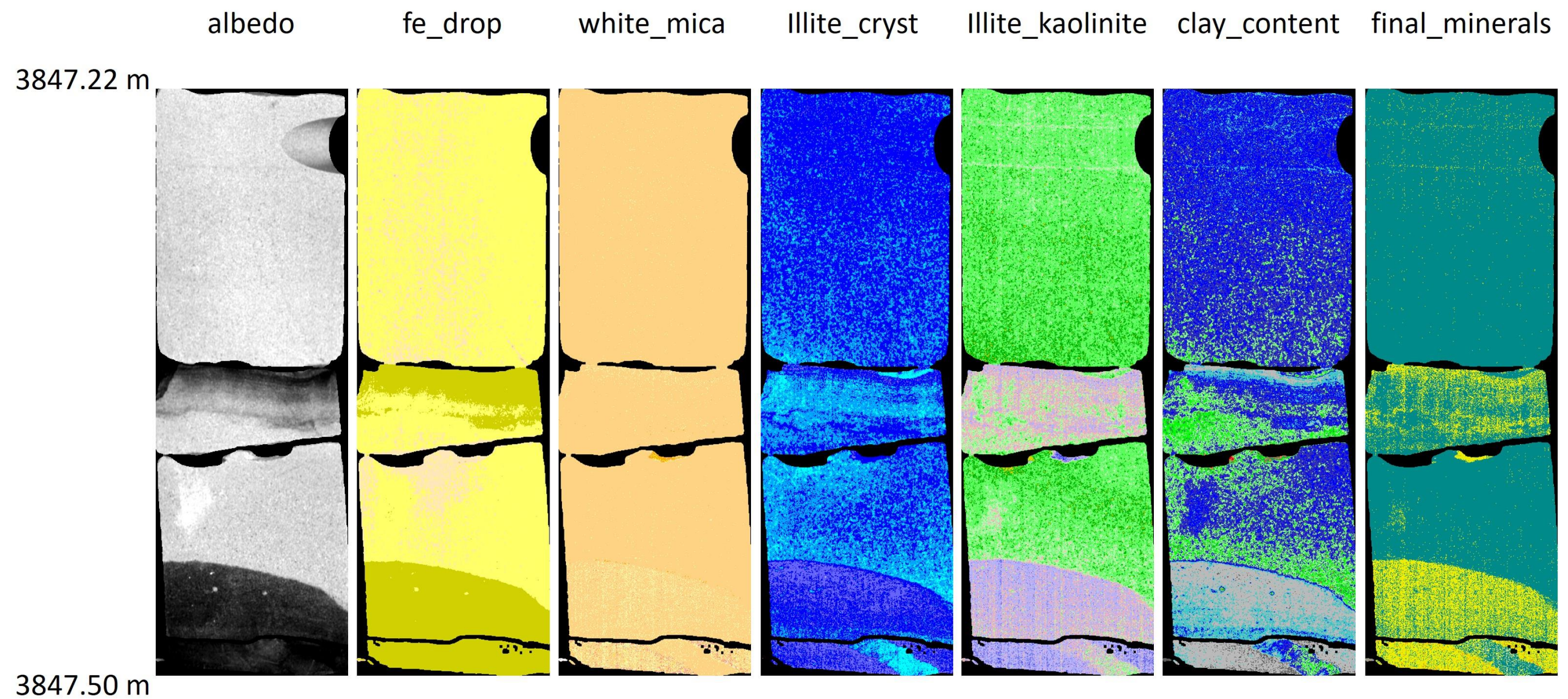


Figure 6: Mineral Map and specific/intermediate tests to understand the character and quantity of the mineral distribution between 3847.22m and 3847.50m.

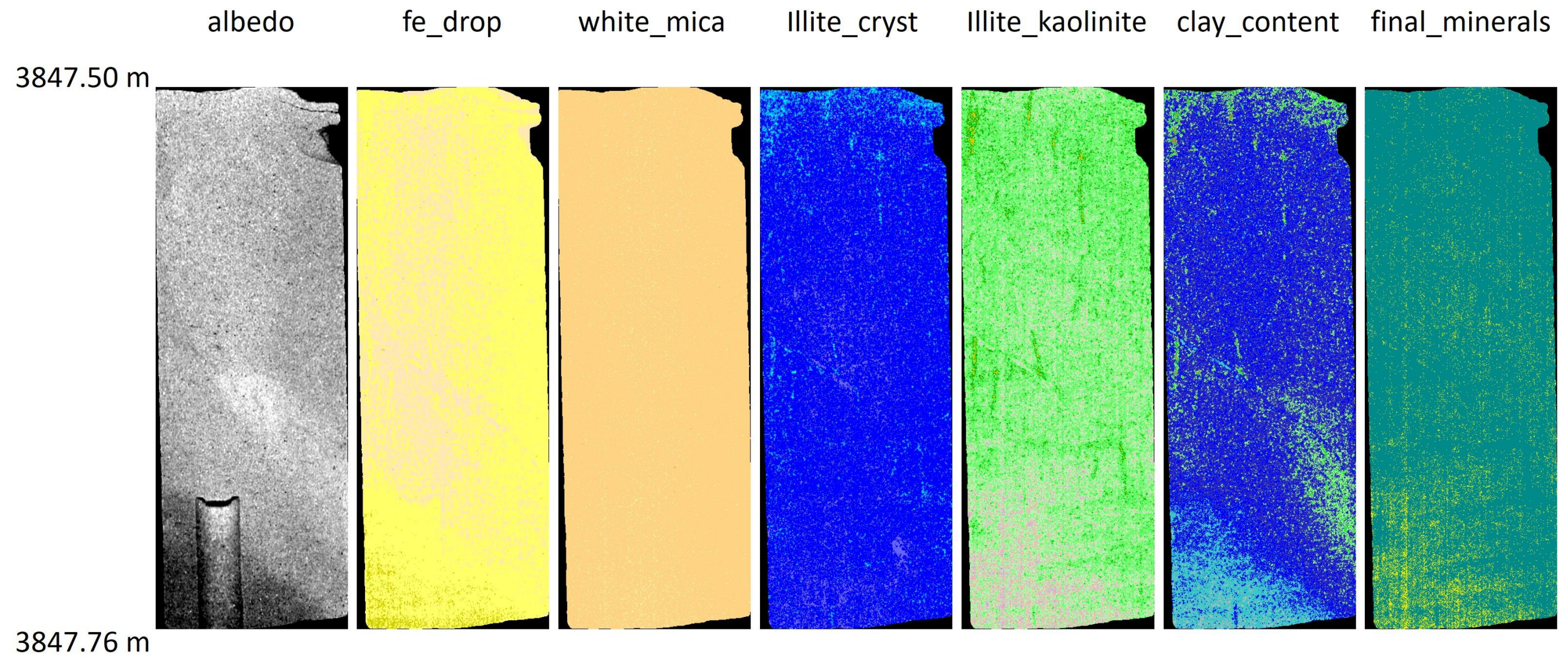


Figure 7: Mineral Map and specific/intermediate tests to understand the character and quantity of the mineral distribution between 3847.50m and 3847.76m.

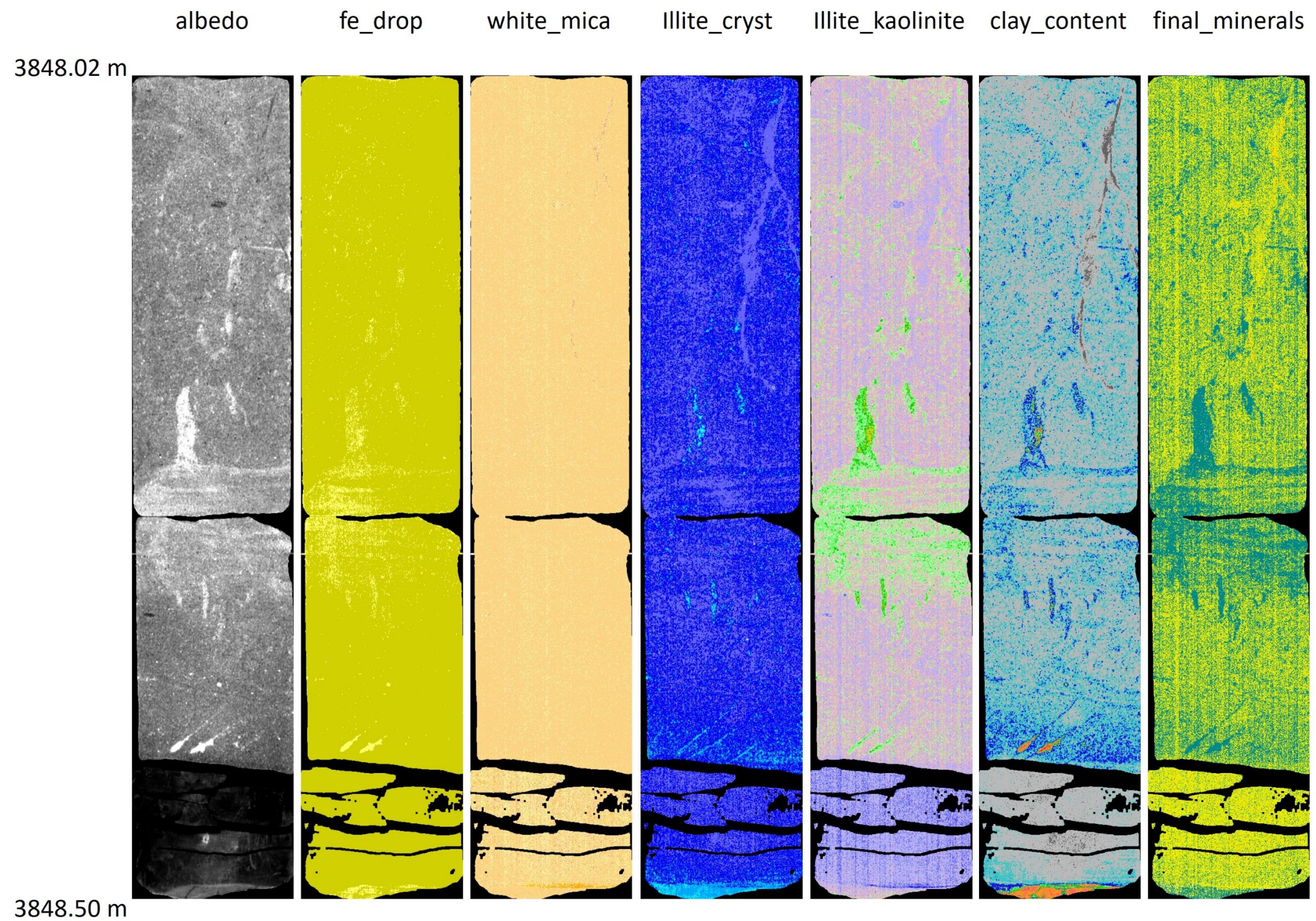


Figure 8: Mineral Map and specific/intermediate tests to understand the character and quantity of the mineral distribution between 3848.02m and 3848.50m.

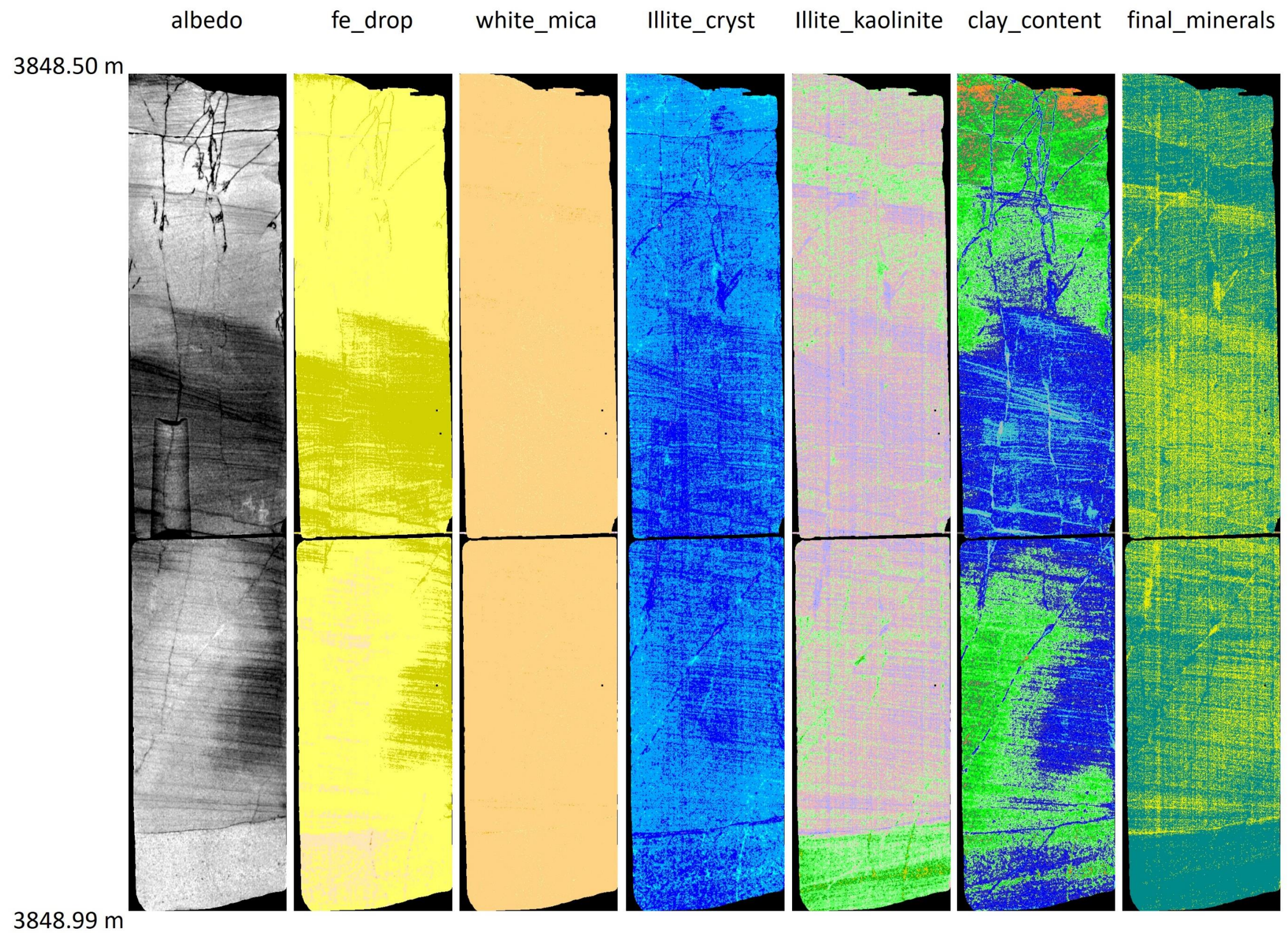


Figure 9: Mineral Map and specific/intermediate tests to understand the character and quantity of the mineral distribution between 3848.50m and 3848.99m.

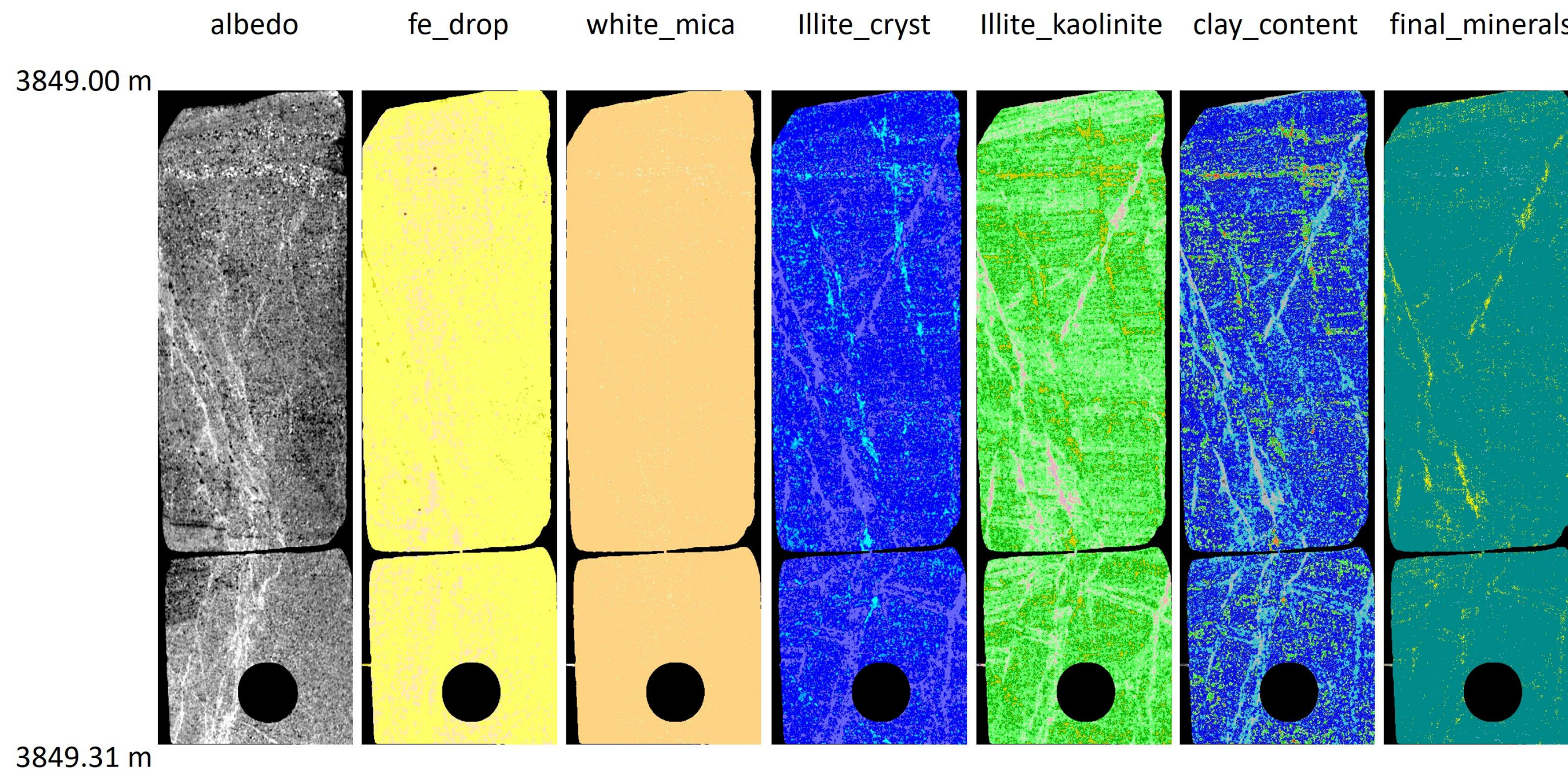


Figure 10: Mineral Map and specific/intermediate tests to understand the character and quantity of the mineral distribution between 3849.00m and 3849.31m.

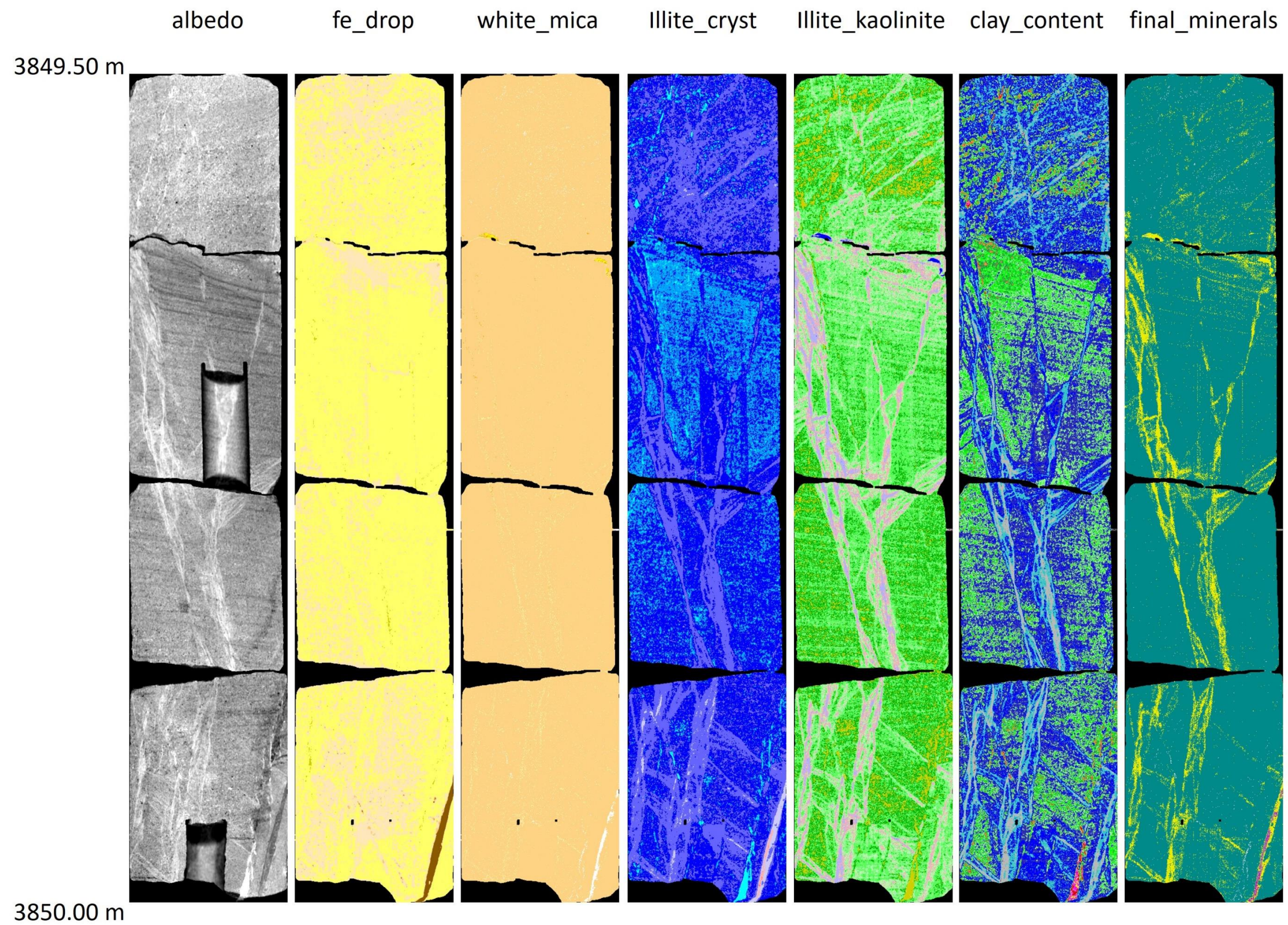


Figure 11: Mineral Map and specific/intermediate tests to understand the character and quantity of the mineral distribution between 3849.50m and 3850.00m.

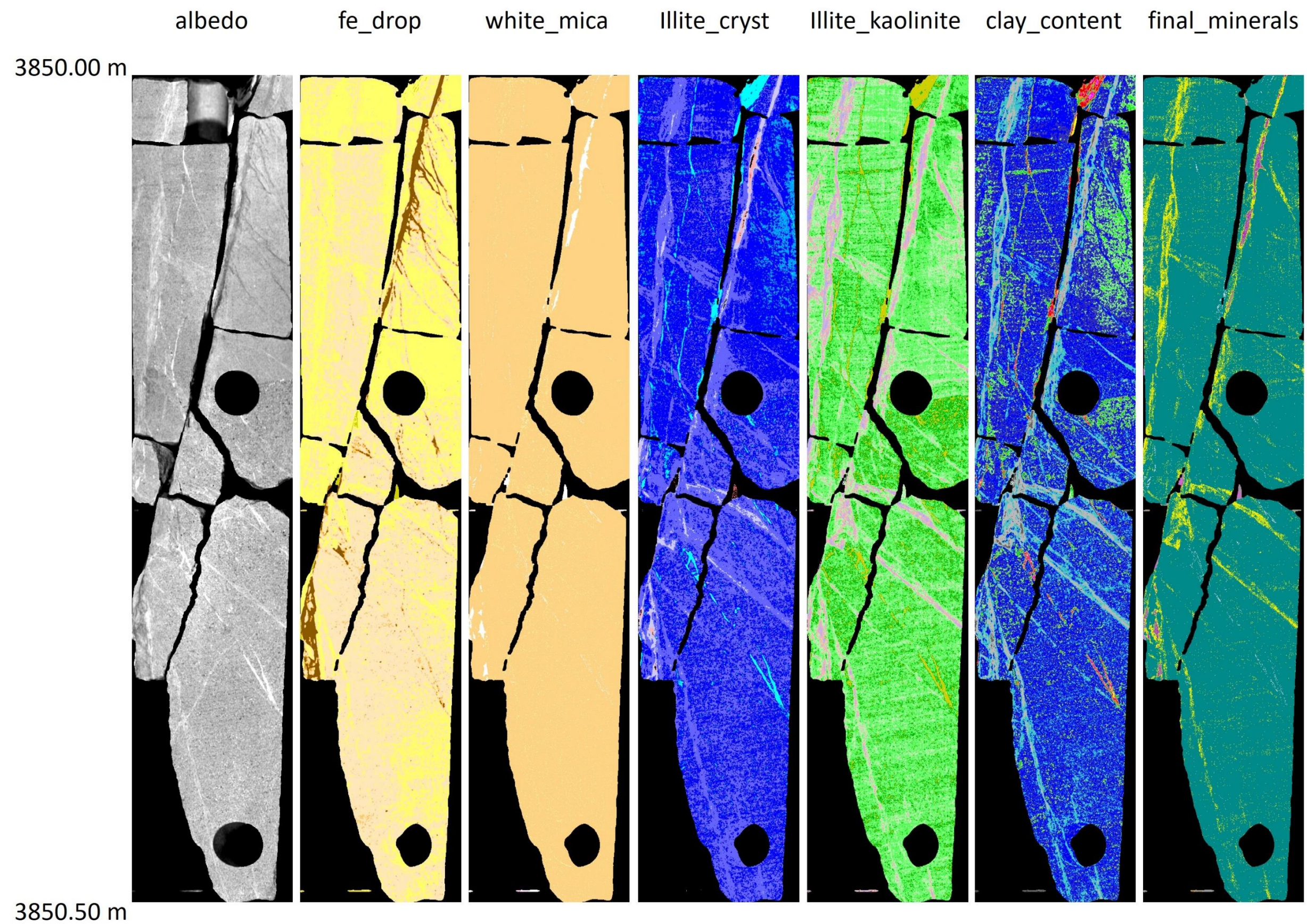


Figure 12: Mineral Map and specific/intermediate tests to understand the character and quantity of the mineral distribution between 3850.00m and 3850.50m.

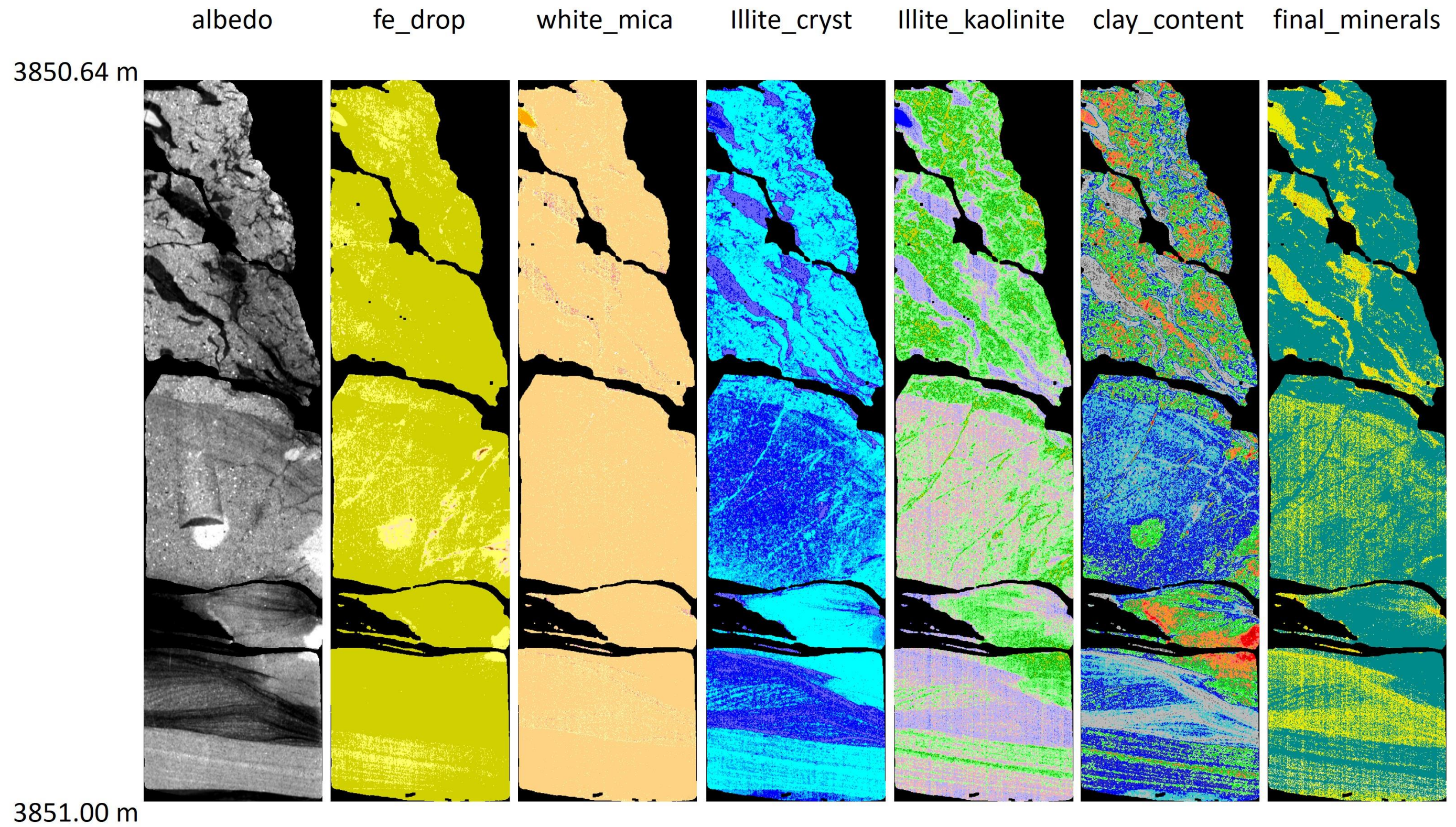


Figure 13: Mineral Map and specific/intermediate tests to understand the character and quantity of the mineral distribution between 3850.64m and 3851.00m.

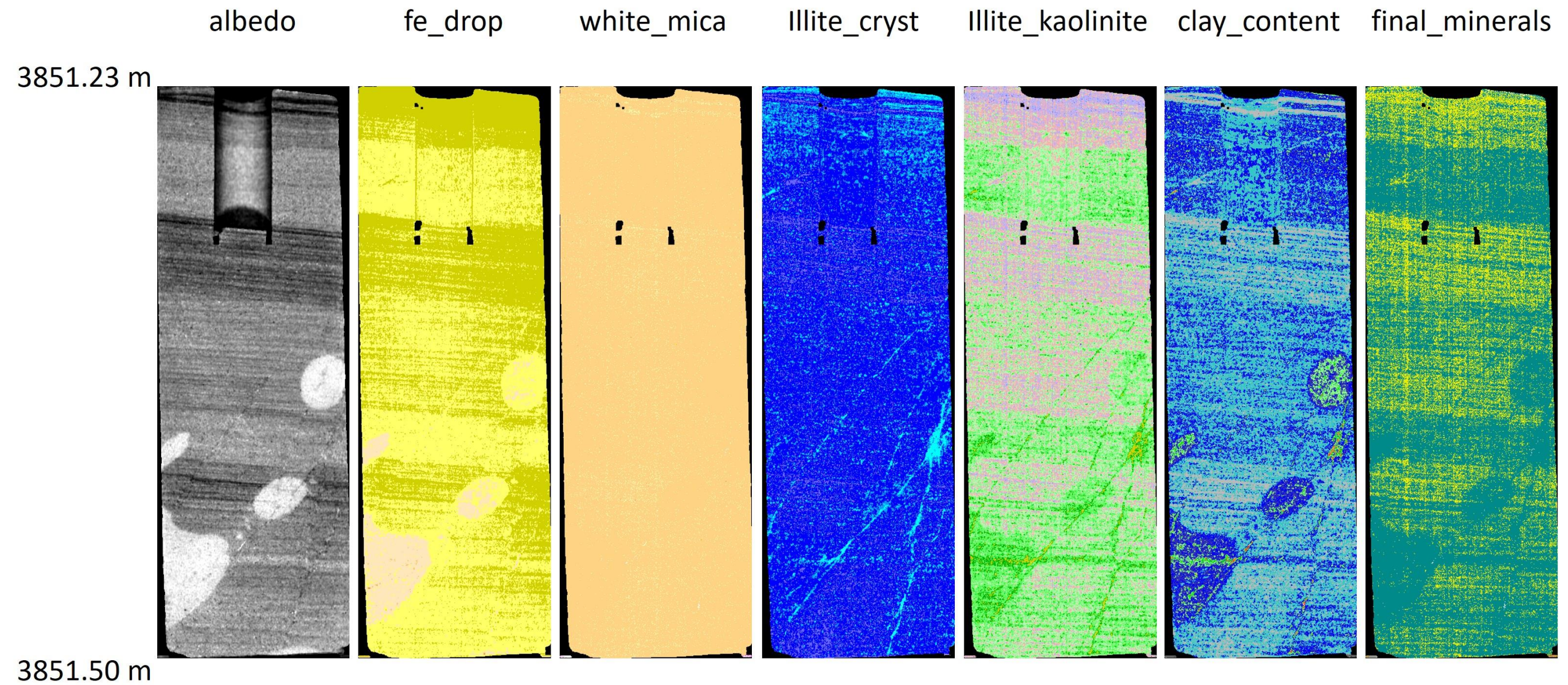


Figure 14: Mineral Map and specific/intermediate tests to understand the character and quantity of the mineral distribution between 3851.23m and 3851.50m.

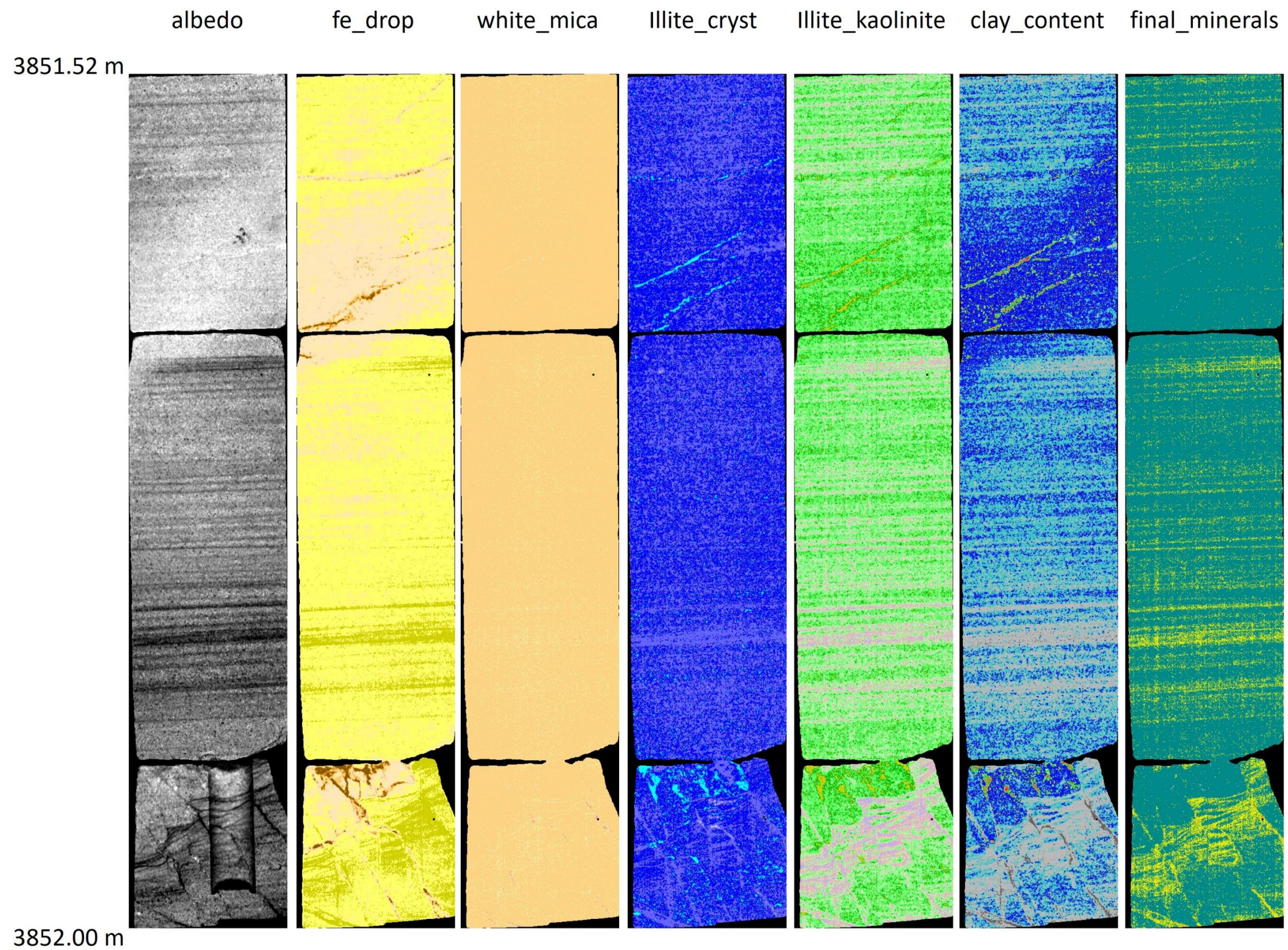


Figure 15: Mineral Map and specific/intermediate tests to understand the character and quantity of the mineral distribution between 3851.52m and 3852.00m.

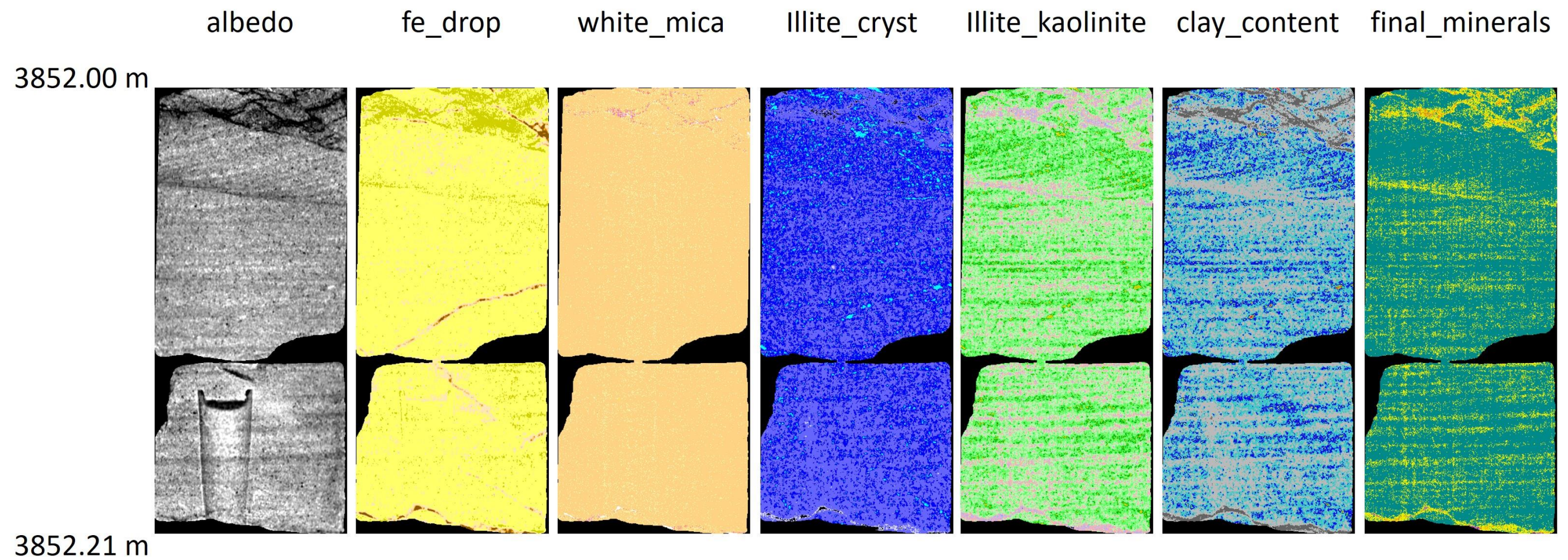


Figure 16: Mineral Map and specific/intermediate tests to understand the character and quantity of the mineral distribution between 3852.00m and 3852.21m.

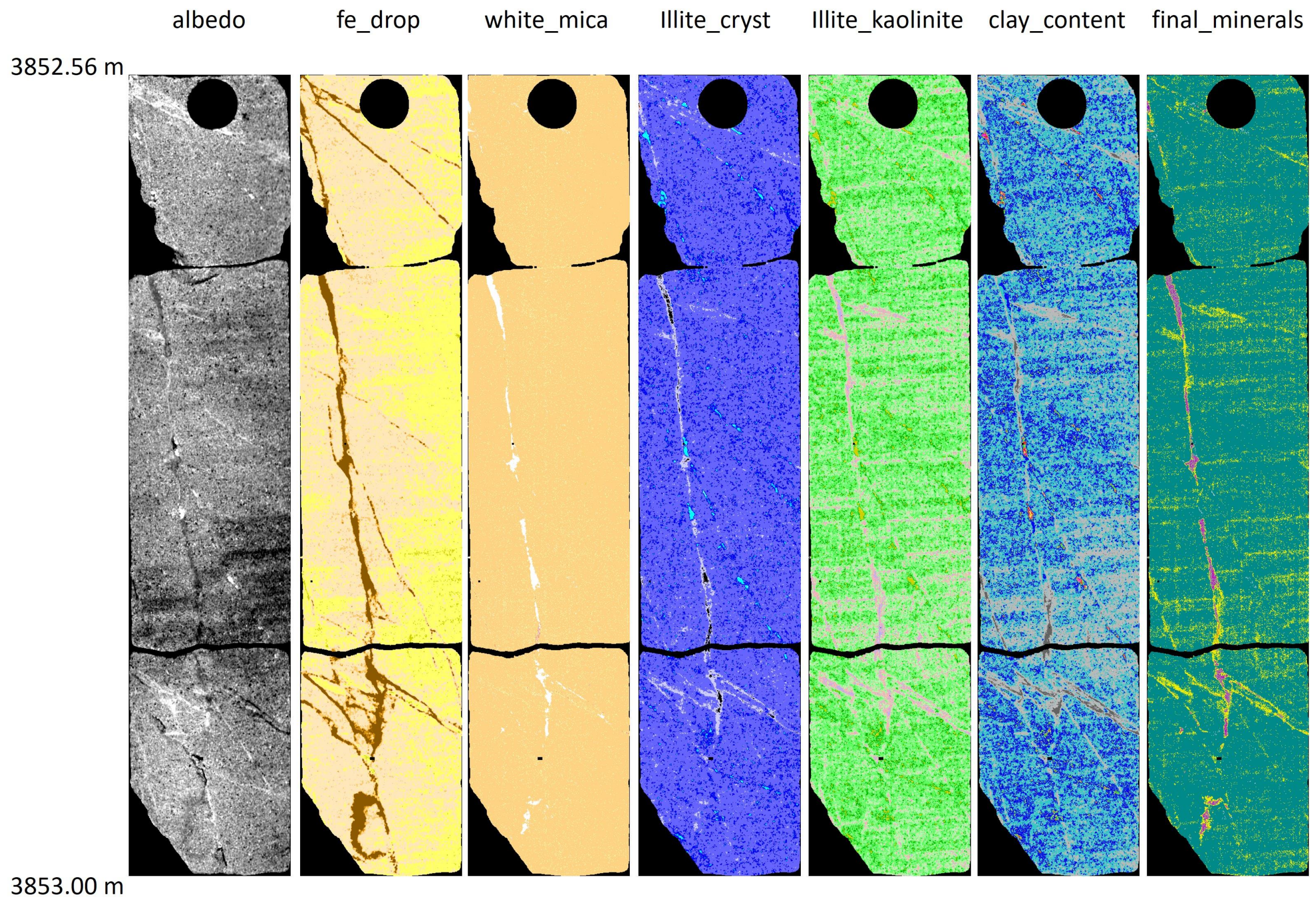


Figure 17: Mineral Map and specific/intermediate tests to understand the character and quantity of the mineral distribution between 3852.56m and 3853.00m.

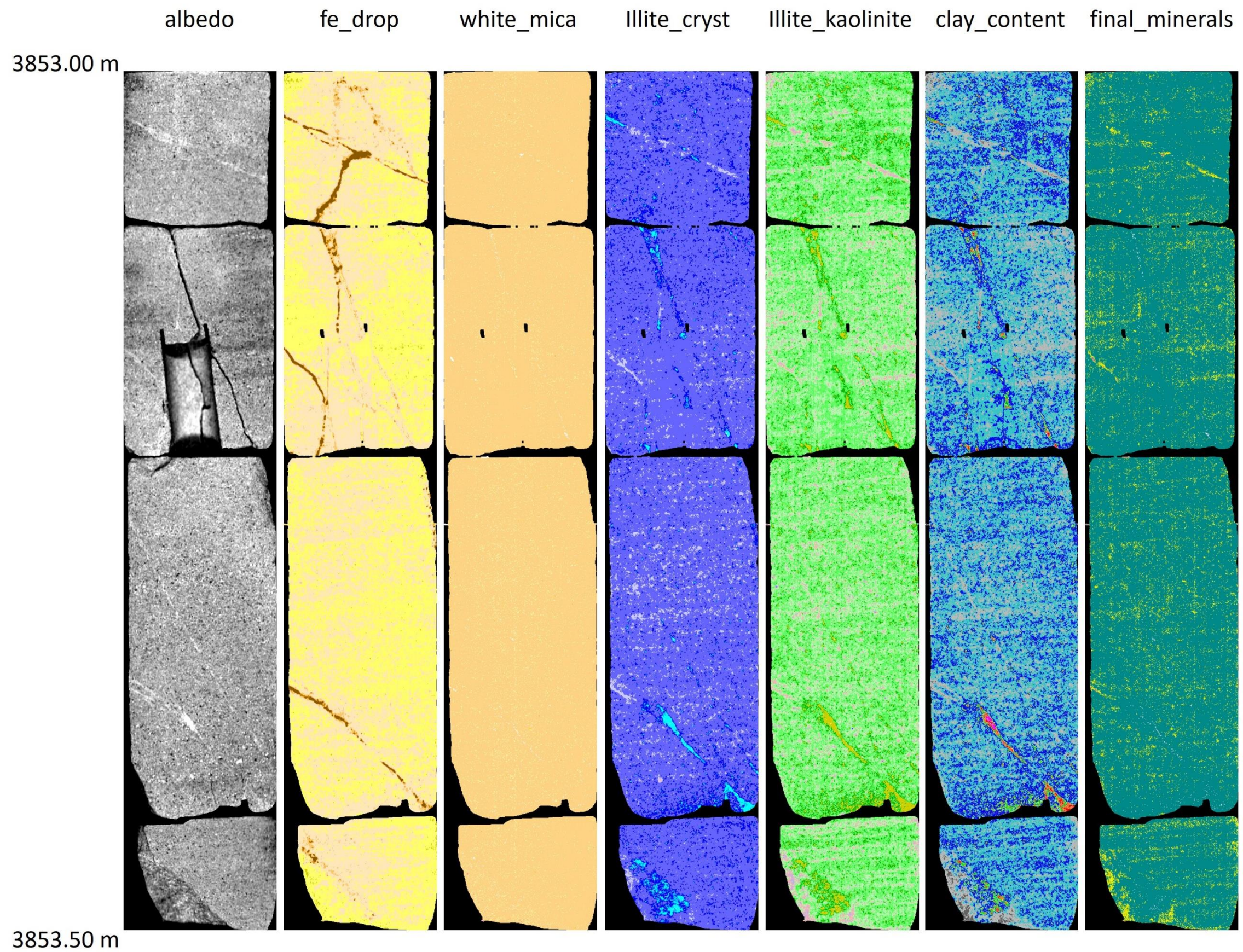


Figure 18: Mineral Map and specific/intermediate tests to understand the character and quantity of the mineral distribution between 3853.00m and 3853.50m.

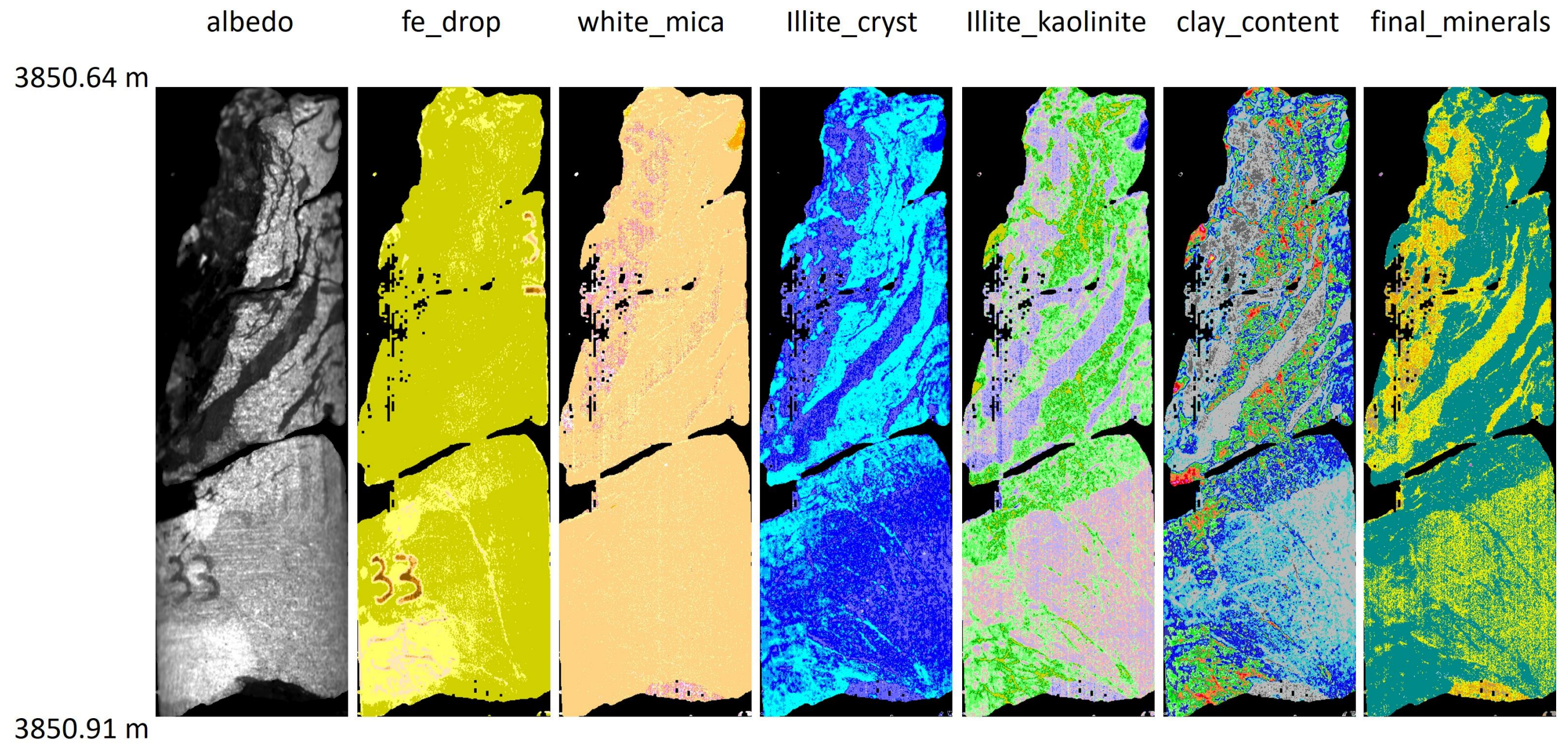


Figure 19: Reverse #1 Mineral Map and specific/intermediate tests to understand the character and quantity of the mineral distribution between 3850.64m and 3850.91m.

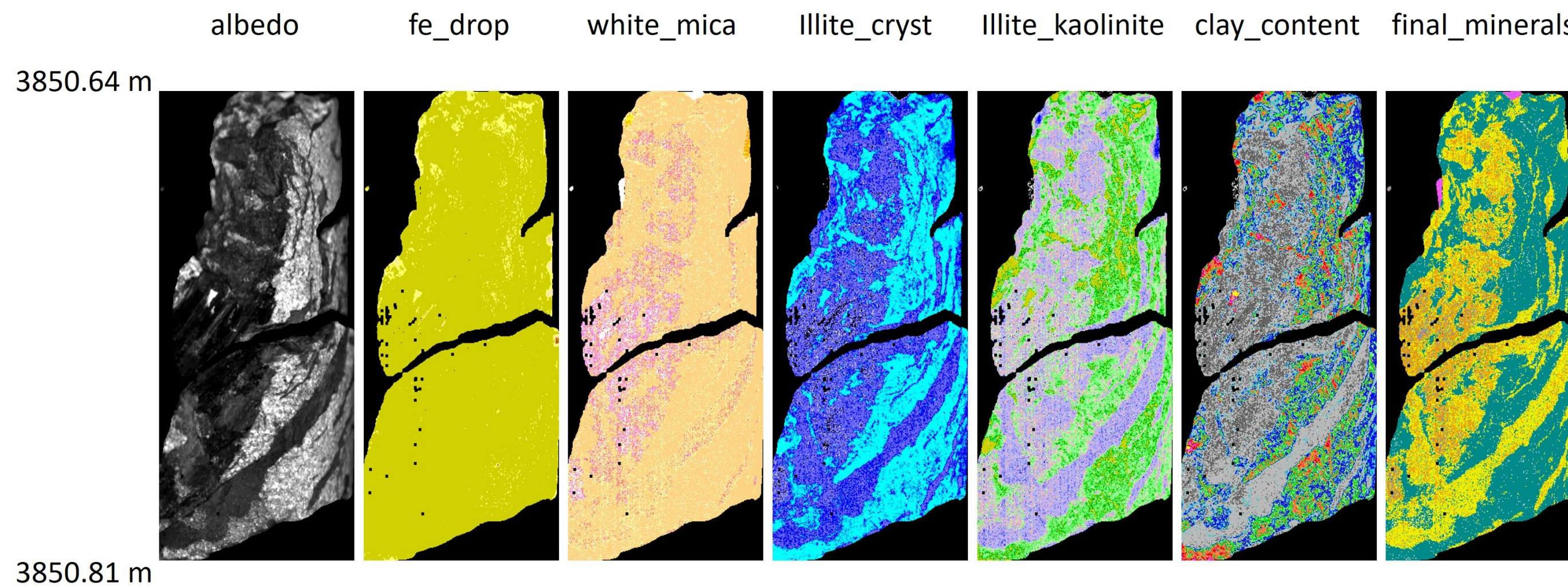










Figure 20: Reverse #2 Mineral Map and specific/intermediate tests to understand the character and quantity of the mineral distribution between 3850.64m and 3850.81m.




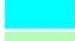






Appendix 3: Hyperspectral Images K05-05

Legend











Fe Drop

name	color
fed-aspectral	
fed-no2100-2400	
fed-low	
fed-med-low	
fed-medium	
fed-med-high	
fed-high	
fed-very-high	









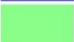










White Mica Composition

name	color
wm-aspectral	
2-LT2185	
wm-LT2190	
wm-LT2190_w2	
wm-LT2195	
wm-LT2195_w2	
wm-LT2200	
wm-LT2200_w2	
wm-LT2205	
wm-LT2205_w2	
wm-LT2210	
wm-LT2210_w2	
wm-LT2215	
wm-LT2215_w2	
wm-LT2220	
wm-LT2220_w2	
wm-LT2225	
wm-LT2225_w2	
wm-GT2225	






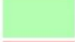




Illite Crystallinity

name	color
ix-aspectral	
ix-NO-ALOH	
ix-smect3	
ix-smect2	
ix-smect1	
ix-smect-ill	
ix-ill-smect	
ix-hx-ill	
ix-musc1	
ix-musc2	

Clay Content (vol%)

name	color
cc-aspectral	
cc-no-ALOH	
cc-0-1	
cc-1-5	
cc-5-10	
cc-10-15	
cc-15-20	
cc-20-25	
cc-25-30	
cc-30-35	
cc-35-40	
cc-40-45	
cc-45-50	
cc-50-60	
cc-60-70	
cc-70-80	
cc-80-90	
cc-90-100	
cc-GT100	

Illite/Kaolinite

name	color
ik-aspectral	
ik-NO-ALOH	
ik-kaol4	
ik-kaol3	
ik-kaol2	
ik-kaol1	
ik-ill1	
ik-ill2	
ik-ill3	
ik-ill4	

Final Minerals

name	color
aspectral	
other<2185nm	
montm-al-rich	
illite-al-rich	
musc-al-rich	
montm	
illite	
musc	
montm-al-poor	
illite-al-poor	
musc-al-poor	
other-2225-2320nm	
dolomite	
fe-dolomite	
ankerite	
fe-ankerite	
calcite	
fe-carbonate	
other>2355nm	
other-chlorite	
kaolinite	
gypsum	

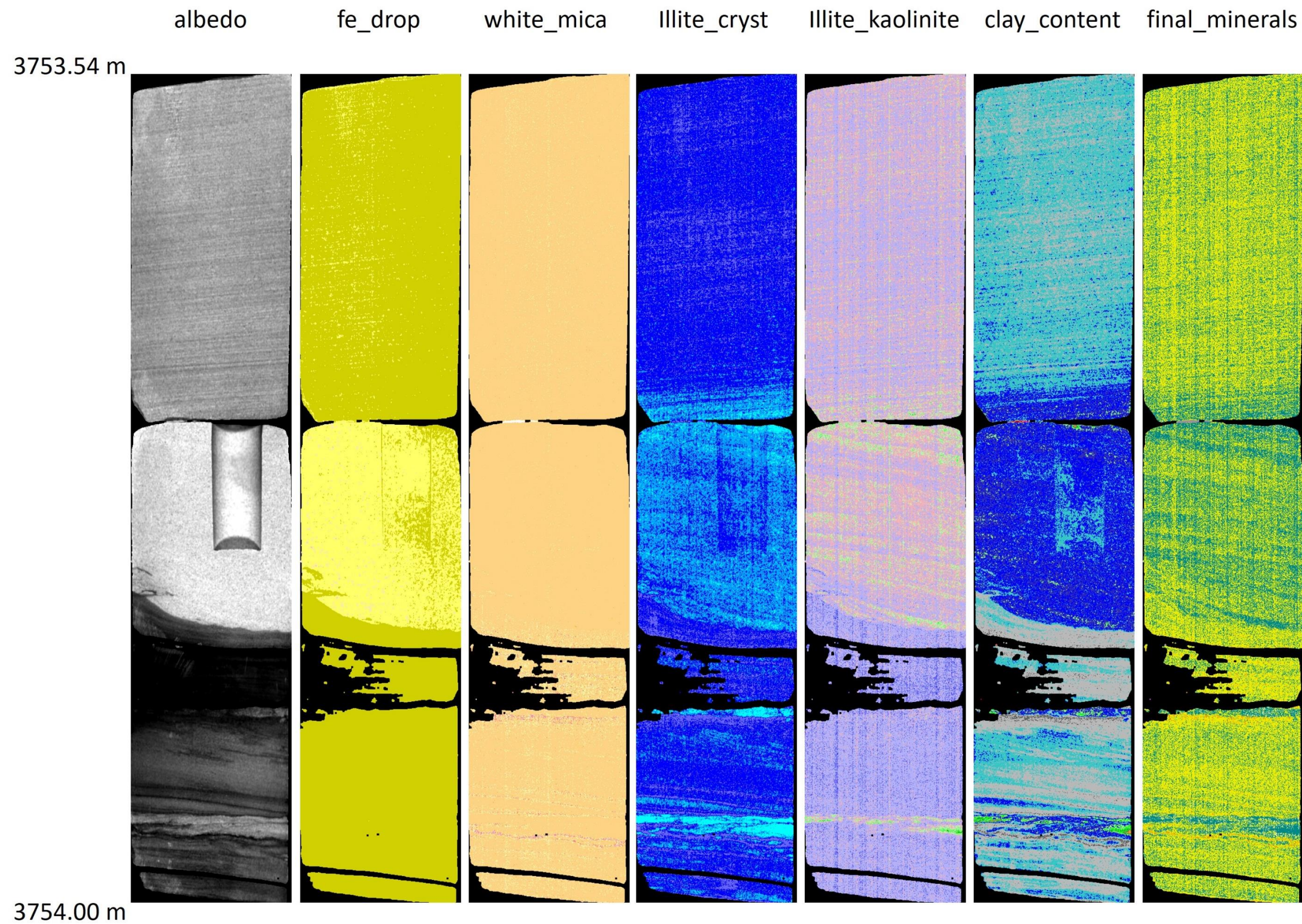


Figure 1: Mineral Map and specific/intermediate tests to understand the character and quantity of the mineral distribution between 3753.54m and 3754.00m.

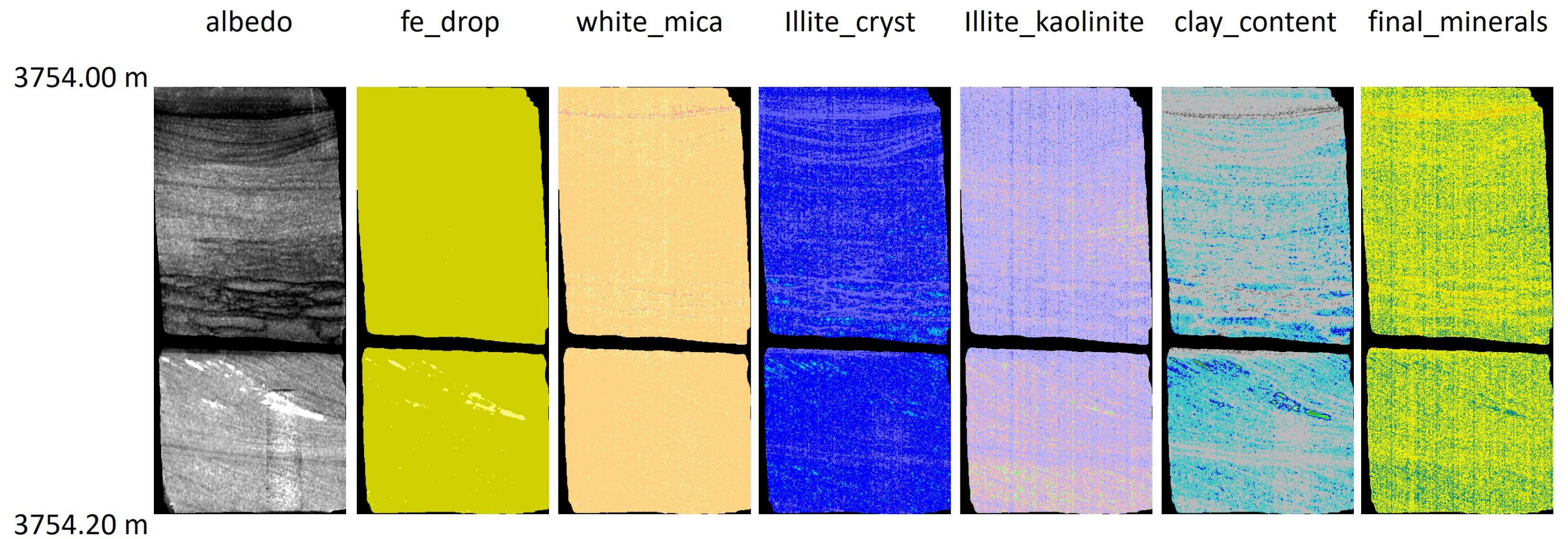


Figure 2: Mineral Map and specific/intermediate tests to understand the character and quantity of the mineral distribution between 3754.00m and 3754.20m.